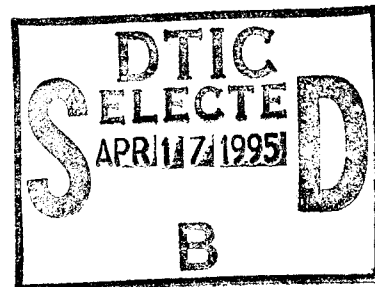


PL-TR-94-2300

## PRELIMINARY ASSESSMENT OF SEISMIC CTBT/NPT MONITORING CAPABILITY

Mark D. Fisk  
Henry L. Gray  
Gary D. McCartor

Mission Research Corporation  
735 State Street  
P.O. Drawer 719  
Santa Barbara, CA 93102-0719



30 November 1994

19950414 088

Scientific Report No. 1

Approved for public release; distribution unlimited




**PHILLIPS LABORATORY**  
**Directorate of Geophysics**  
**AIR FORCE MATERIEL COMMAND**  
**HANSCOM AIR FORCE BASE, MA 01731-3010**

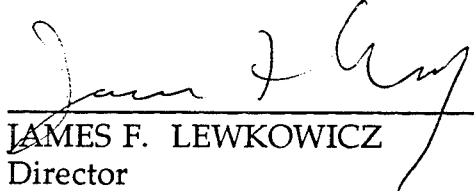
SPONSORED BY  
Advanced Research Projects Agency (DoD)  
Nuclear Monitoring Research Office  
ARPA ORDER No. A-128

MONITORED BY  
Phillips Laboratory  
CONTRACT No. F19628-93-C-0117

The views and conclusions contained in this document are those of the authors and should not be interpreted as representing the official policies, either express or implied, of the Air Force or the U.S. Government.

This technical report has been reviewed and is approved for publication.

  
JAMES F. LEWKOWICZ  
Contract Manager  
Earth Sciences Division

  
JAMES F. LEWKOWICZ  
Director  
Earth Sciences Division

This report has been reviewed by the ESC Public Affairs Office (PA) and is releasable to the National Technical Information Service (NTIS).

Qualified requestors may obtain additional copies from the Defense Technical Information Center. All others should apply to the National Technical Information Service.

If your address has changed, or if you wish to be removed from the mailing list, or if the addressee is no longer employed by your organization, please notify PL/IM, 29 Randolph Road, Hanscom AFB, MA 01731-3010. This will assist us in maintaining a current mailing list.

Do not return copies of this report unless contractual obligations or notices on a specific document requires that it be returned.

<b>REPORT DOCUMENTATION PAGE</b>			<i>Form Approved</i> <b>OMB NO. 0704.0188</b>	
Public reporting burden for this collection of information is estimated to average 1 hour per response, including the time for reviewing instructions, searching existing data sources, gathering and maintaining the data needed, and completing and reviewing the collection of information. Send comments regarding this burden estimate or any other aspect of the collection of information, including suggestions for reducing this burden, to Washington Headquarters Services, Directorate for Information Operations and Reports, 1215 Jefferson Davis Highway, suite 1204, Arlington, VA 22202-4302, and to the Office of Management and Budget, Paperwork Reduction Project (0704-0188), Washington, DC 20503.				
1. AGENCY USE ONLY (Leave Blank)		2. REPORT DATE 30 Nov 1994	3. REPORT TYPE AND DATES COVERED Scientific Report No. 1	
4. TITLE AND SUBTITLE Preliminary Assessment of Seismic CTBT/NPT Monitoring Capability			5. FUNDING NUMBERS  PE62301E	
6. AUTHOR(s) Mark D. Fisk Henry L. Gray* Gary D. McCartor*			PRNM93 TAGM WUAL Contract F19628-93-C-0117	
7. PERFORMING ORGANIZATION NAME(S) AND ADDRESS(ES) Mission Research Corporation 735 State Street, P.O. Drawer 719 Santa Barbara, CA 93102-0719			8. PERFORMING ORGANIZATION REPORT NUMBER  MRC-R-1484	
9. SPONSORING/MONITORING AGENCY NAME(S) AND ADDRESS(ES) Phillips Laboratory Hanscom Air Force Base Massachusetts 01731-3010 Attn: James Lewkowicz/GPEH			10. SPONSORING/MONITORING AGENCY REPORT NUMBER  PL-TR-94-2300	
11. SUPPLEMENTARY NOTES  * Southern Methodist University, Dallas, TX				
12a. DISTRIBUTION/AVAILABILITY STATEMENT  Approved for public distribution; distribution unlimited			12b. DISTRIBUTION CODE	
13. ABSTRACT (Maximum 200 words)  Our recent work focuses on assessing seismic event identification performance using a method we developed for outlier detection. This is motivated by the lack of seismic calibration data for underground nuclear explosions in most regions and the difficulty associated with transporting regional discriminants. The procedure may be fully automated to flag events warranting special attention and to test all appropriate assumptions to ensure validity. The method also allows control of false alarm rates and a natural way to rank events. The procedure is applied to nuclear explosions, earthquakes, mining blasts and mine tremors in diverse geological regions, recorded by the ARCESS and GERESS arrays, CDSN station WMQ, and LNN stations KNB and MNV. Discriminants used include Pn/Lg and Pn/Sn in several frequency bands from 3 to 8 Hz, as well as Lg spectral ratios. Identification and false alarm rates were estimated for each region using a standard set of discriminants. At 0.01 significance level, between 92-100% of the explosions and quarry blasts were detected as outliers of the earthquake groups in the various regions, except at KNB where the outlier detection rate was 80%. There were 3 false alarms out of 158 earthquakes, slightly higher than the target rate of 1%.  Effects of contaminated training data were also studied by intentionally including quarry blasts or rock bursts in earthquake training sets to determine if the outlier test can detect them and to assess potential impacts on monitoring performance. Pn/Lg transportability was also examined to assess how precisely a discrimination threshold must be transported in order to be effective. Last, identification analysis of the 31 December 1992 Novaya Zemlya event was repeated after first applying distance corrections.				
14. SUBJECT TERMS Seismic Discrimination Outlier Detection Regional Arrays			15. NUMBER OF PAGES 50	
Comprehensive Test Ban Treaty Classification Attenuation Corrections			16. PRICE CODE	
17. Security CLASSIFICATION OF REPORT UNCLASSIFIED	18. Security CLASSIFICATION OF THIS PAGE UNCLASSIFIED	19. Security CLASSIFICATION OF ABSTRACT UNCLASSIFIED	20. LIMITATION OF ABSTRACT SAR	

UNCLASSIFIED

SECURITY CLASSIFICATION OF THIS PAGE

CLASSIFIED BY:

DECLASSIFY ON:

SECURITY CLASSIFICATION OF THIS PAGE

UNCLASSIFIED

## Table of Contents

1. Introduction .....	1
2. Seismic Data Sets and Regional Discriminants .....	3
2.1. WMQ Data Set .....	5
2.2. ARCESS Data Set .....	8
2.3. GERESS Data Set .....	11
2.4. KNB and MNV Data Sets .....	12
2.5. Data Set Comparisons and Pn/Lg Transportability .....	17
3. Technical Approach .....	19
3.1. Motivation .....	19
3.2. Outlier Detection Approach .....	20
3.3. Classification Approach .....	21
4. Monitoring Applications .....	22
4.1. Applications of the Outlier Test .....	22
4.2. Contaminated Training Set Study .....	27
4.3. Applications with the Classification Test .....	29
4.4. Identification Results for the 921231 Novaya Zemlya Event .....	32
5. Conclusions and Recommendations .....	35
References .....	36

Accession For	
NTIS GRA&I	<input checked="" type="checkbox"/>
DTIC TAB	<input type="checkbox"/>
Unannounced	<input type="checkbox"/>
Justification -	
By	
Distribution	
Availability Codes	
Dist	Avail and/or Special
A-1	

## List of Figures

1. Locations of the ARCESS and GERESS arrays, CDSN station WMQ, LNN stations KNB and MNV, and most of the seismic events used in our regional event identification study. .... 3
2. Locations of CDSN station WMQ, 16 nuclear explosions in Kazakhstan, the 880929 nuclear explosion at Lop Nor and 23 earthquakes in China and nearby countries..... 5
3. Scatter plots of Pn/Lg (left) and Pg/Lg (right) in nine frequency bands, before applying distance corrections, for 17 nuclear explosions and 23 earthquakes recorded by station WMQ. .... 6
4. Plots of uncorrected (left) and distance-corrected (right) Pn/Lg values in the 6-8 Hz band versus epicentral distance for WMQ events. .... 6
5. Scatter plots of Pn/Lg (left) and Pg/Lg (right) in nine frequency bands, after applying distance corrections, for 17 nuclear explosions and 23 earthquakes recorded by station WMQ. .... 7
6. Scatter plots of Lg spectral ratios for nuclear explosions and earthquakes recorded by WMQ, based on maximum (left) and rms (right) measurements of Lg spectra in three combinations of frequency bands on the sz channel. .... 8
7. Locations of the ARCESS, GERESS and NORESS arrays and events used in this study. .... 9
8. Scatter plots of Pn/Lg in nine frequency bands, before (left) and after (right) applying distance corrections, for 53 quarry blasts on the Kola Peninsula, 39 quarry blasts in the Kiruna region in Sweden and 24 earthquakes near Steigen, Norway, recorded by the ARCESS array. .... 10
9. Scatter plots of Pn/Sn in six frequency bands, before (left) and after (right) applying distance corrections, for 53 Kola and 2 Kiruna quarry blasts, 24 Steigen and 5 Spitsbergen earthquakes, 3 Novaya Zemlya nuclear explosions, and the 921231 Novaya Zemlya event, recorded by ARCESS. .... 10
10. Scatter plots of Pn/Lg (left) and Pn/Sn (right) in nine frequency bands for 13 quarry blasts, 10 earthquakes and 30 rock bursts recorded by the GERESS array. .... 11
11. Lg spectral ratios for earthquakes, quarry blasts and rockbursts recorded by GERESS, based on maximum (left) and rms (right) measurements in three combinations of frequency bands. .... 12
12. Map of the southwestern U.S. showing locations of LNN stations KNB and MNV relative to NTS. On the left is an enlarged map of NTS showing epicenters of the nuclear explosions and earthquakes used in this study. (Courtesy of W. Walter of LLNL.) .. 13

13. Scatter plots of Pn/Lg and Pg/Lg measurements in the 6-8 Hz band for seismic events recorded by LNN stations KNB and MNV. ....	14
14. Pn/Lg measurements in the 6-8 Hz band versus ML(coda) for events recorded by KNB (left) and MNV (right). ....	15
15. Scatter plots of Lg spectral ratio measurements of three different types for seismic events recorded by LNN stations KNB and MNV. Events are separated into subgroups as in Figure 13. ....	16
16. Spectral ratio (1-2 Hz/6-8 Hz) measurements of Lg coda versus ML(coda) for events recorded by KNB (left) and MNV (right). Lg spectral ratios exhibit significant magnitude dependence and do not discriminate earthquakes and explosions in this region below ML 3.5. ....	16
17. Uncorrected (left) and distance-corrected (right) Pn/Lg(6-8 Hz) for events recorded by ARCESS, GERESS, WMQ, MNV and KNB. Horizontal lines depict discrimination thresholds for each station. ....	19
18. Summary of outlier test results (detection and false alarm rates) at ARCESS, GERESS, WMQ, MNV and KNB. Overall results are shown on the far right. ....	23
19. Graphical representation of outlier test results for the WMQ events. The triangles and circles show values of the likelihood ratio for the explosions and earthquakes being tested, respectively. Events whose likelihood ratios are less than the threshold (vertical line) are identified as outliers. ....	24
20. Graphical representations of outlier test results for Novaya Zemlya nuclear explosions (upper left), Kola quarry blasts (upper right), Kiruna quarry blasts (lower left), and Vogtland quarry blasts (lower right). The triangles depict values of the likelihood ratio for the explosions while the circles correspond to values of the likelihood ratio for the earthquakes considered at each array. ....	25
21. Outlier test results for MNV events with both discriminant values present. The triangles and circles show values of the likelihood ratio for the explosions and earthquakes being tested, respectively. ....	26
22. Same as Figure 21 but for events recorded by KNB with both discriminant values present. ....	27
23. Graphical representation of classification results for 78 NTS nuclear explosions (triangles) and 37 earthquakes (circles) recorded by MNV. All events were classified correctly. ....	30
24. Graphical representation of classification results for 89 NTS nuclear explosions (triangles) and 59 earthquakes (circles) recorded by KNB. In this case, 75 of 89 explosions and 58 of 59 earthquakes were classified correctly. ....	31

25. Summary of classification results at ARCESS, GERESS, WMQ, MNV and KNB. Results are expressed in terms of the percentage of explosions correctly classified and the false alarm rate at each station. Overall results are shown on the far right. .... 31
26. Locations of the 921231 event (ORID=361575) on Novaya Zemlya, reference events used in its identification analysis, and the ARCESS array at which all events were recorded. .... 33

## List of Tables

1. Summary of seismic data sets used in our study. .... 4



## 1. Introduction

Objectives for an international CTBT (Comprehensive Test Ban Treaty) monitoring system, stated in the United States Working Paper for the Committee on Disarmament (May 18, 1994), are detection and identification of nuclear explosions down to a few kilotons or less. Difficulties associated with seismic event identification down to this level include the fact that small events may be seen at only a single station and, annually, there are many thousands of competing earthquakes, mining blasts and other mining-induced events worldwide. Thus, robust automated methods are needed to make use of limited information and to reduce the workload of human analysts to a manageable level.

Furthermore, observed seismic signals from small sources are generally quite complicated and exhibit dramatic dependence on regional geophysics; even the most promising discriminants can vary widely in different region. Hence, region-specific information regarding seismic discriminants is vital in distinguishing nuclear explosions from other events. Unfortunately, relevant ground-truth data, particularly for small underground nuclear explosions, do not exist for most regions, including many of current interest. In addition, it has yet to be shown that discrimination rules, established in a given region for which data exist, can be transported effectively to a new region. Thus, in most cases, seismic event identification, within the context of CTBT or NPT (Non-Proliferation Treaty) monitoring, is a problem of detecting unusual events, i.e., outliers.

In addition, precise statistical metrics are needed to quantify identification performance to meet the specific needs of policy use. In this regard, good control of the one of the error rates is needed so that the false alarm rate, for example, is not overwhelming and, if there is an alert, the probability that an error was made is known precisely. It may further be desirable to rank events in order to focus on the most "suspicious" ones.

Thus this effort has concentrated on developing and applying statistical methods to perform seismic event identification and on quantifying identification capabilities with regard to seismic monitoring of a CTBT or NPT. We have been developing and applying a statistical framework for seismic event identification with these and other considerations in mind.

The fundamental methods consist of statistical tests for outlier detection and classification, as well as preliminary statistical analyses to test appropriate assumptions regarding the data in order to optimize the results and ensure self-consistency. Our methodology provides a statistical framework for seismic event identification that: (1) accurately treats statistical

fluctuations of all discriminants used; (2) can identify nuclear tests in regions for which relevant ground-truth training data may or may not exist; (3) provides flexibility to incorporate any discriminant and assess its utility objectively; (4) can function in an automated mode to flag and/or rank suspicious events; (5) can control the false alarm rate; (6) precisely quantifies identification performance; (7) and provides a rigorous and defensible framework with which to report and justify the results. To also serve as an interactive analyst and research tool, we have been developing an X Window graphical user interface, featuring a wide range of graphical displays and exploratory data analysis tools.

Our recent work has focused on assessing regional event identification capabilities using a method we developed for outlier detection. This is motivated by the fact that historical underground nuclear tests have been performed in only a few regions. Our procedure may be fully automated to flag events warranting special attention and to test all appropriate assumptions to ensure validity of the results. In addition, the method allows straightforward control of false alarm rates and a natural way to rank events. We have applied this approach to seismic events in diverse geological regions, recorded by the ARCESS and GERESS arrays in Norway and Germany, CDSN (Chinese Digital Seismic Network) station WMQ in China, and LNN (Livermore NTS Network) stations KNB and MNV in the western U.S.

We have also examined effects of contaminated training data by intentionally including quarry blasts or rock bursts in earthquake training sets to determine if the outlier test can detect them and to assess potential impacts on monitoring performance. We also used our classification test to identify these events to illustrate how it can be used to improve identification performance for cases in which more than one training set exist. Last, we repeated our identification analysis of the 31 December 1992 Novaya Zemlya event, after first applying distance corrections.

In Section 2, we describe ground-truth data sets from ARCESS, GERESS, WMQ, KNB and MNV, which we use as a testbed to assess regional event identification performance. We describe which discriminants perform robustly in the various regions and provide a comparison of Pn/Lg among the regions. In Section 3, we describe the procedures for outlier detection and for event classification. The latter approach applies to cases for which training data for more than one event type exist for a given region. In Section 4, we present results of monitoring applications. In Section 5, we discuss conclusions regarding the current status of regional identification performance using our statistical framework and provide recommendations for future research and development efforts.

## 2. Seismic Data Sets and Regional Discriminants

For this study we used feature (i.e., discriminant) data provided by Baumgardt (1993a) for seismic events recorded by the ARCESS and GERESS regional arrays and CDSN (Chinese Digital Seismic Network) station WMQ. ARCESS events include 24 earthquakes (EQs) near Steigen, Norway, 5 earthquakes near Spitsbergen, 53 quarry blasts (QBs) on the Kola Peninsula, 39 quarry blasts in the Kiruna region of Sweden, and 3 underground nuclear explosions (EXs) at the Novaya Zemlya test site. GERESS events include 10 earthquakes and 13 quarry blasts in the Vogtland region of western Bohemia (straddling Germany and the Czech Republic) and 30 rock bursts (RBs) in the Lubin region of Poland. (The Steigen, Vogtland and Lubin data sets are included in the CSS Ground-Truth Database and are discussed in more detail by Grant et al., 1993.) WMQ events include 23 earthquakes in China and nearby countries, 16 nuclear explosions in Kazakhstan, and 1 nuclear explosion at the Lop Nor test site in China. In addition, we also used feature data provided by Patton and Walter (1994) for 76 earthquakes and 141 nuclear explosions at NTS (Nevada Test Site), recorded by LNN (Livermore NTS Network) stations KNB and MNV. Figure 1 depicts locations of the seismic stations, arrays and most of the events considered in this study. Table 1 summarizes the events, their epicentral distances and magnitudes.

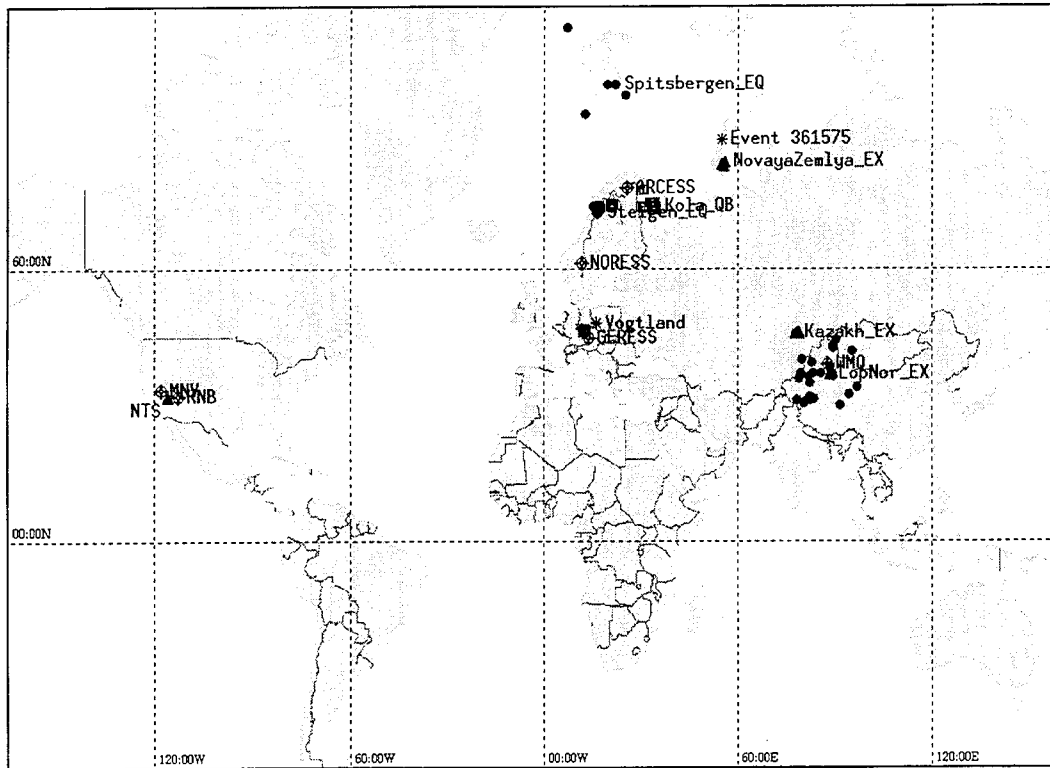


**Figure 1. Locations of the ARCESS and GERESS arrays, CDSN station WMQ, LNN stations KNB and MNV, and most of the seismic events used in our regional event identification study.**

A significant aspect of this combined data set is its diversity. First, the geological regions represented here are very diverse. In fact, geologies of the western U.S. and Scandinavia are dramatically (if not extremely) different. Second, epicentral distances range from 100 to 1300 km, covering nearly the full range of what are considered regional distances. Third, the events have a broad range of magnitudes from 1.0 to 6.1. Fourth, there are different types of events which were nearly collocated, such as the events recorded by GERESS and, to some extent, those recorded by KNB and MNV. There are also stations, such as WMQ, for which events were observed for a full range of distances and azimuths. Last, the types and configurations of seismic instrumentation differ. ARCESS and GERESS are regional arrays (Mykkeltveit et al., 1990; Harjes, 1990), while WMQ, MNV and KNB are each single stations. Thus, the combined data set provides a broad characteristic sample of the types of regional events that will be encountered when monitoring a CTBT.

**Table 1: Summary of seismic data sets used in our study.**

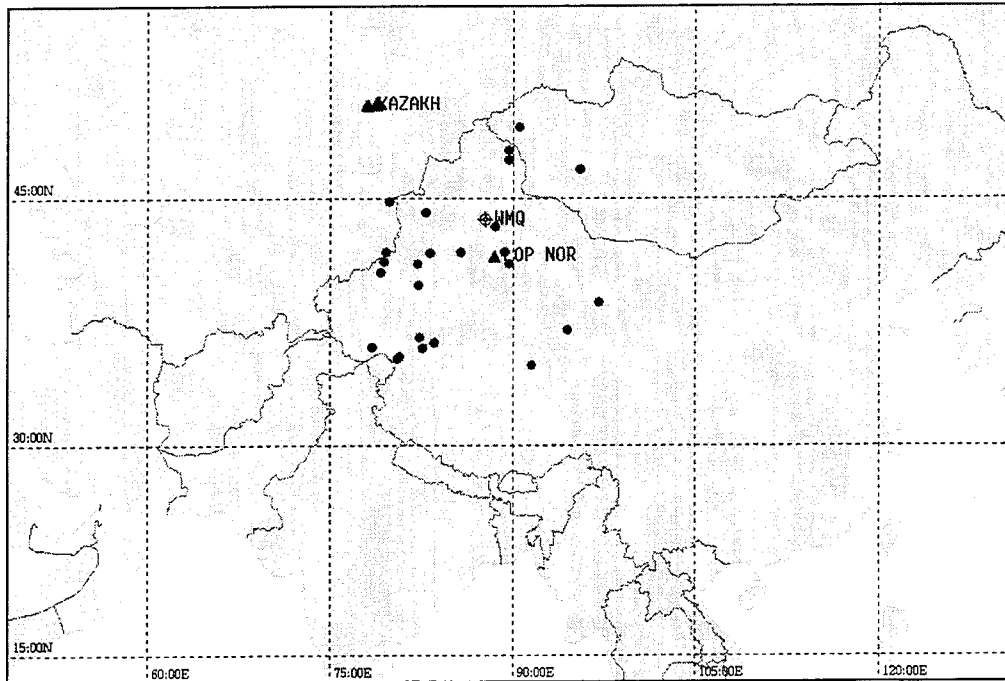
Array/Station	Events	Distance (km)	Magnitude
ARCESS	24 Steigen EQs	385-480	1.0-3.2
	5 Spitsbergen EQs	795-1320	1.5-2.9
	53 Kola QBs	300-430	2.0-3.2
	39 Kiruna QBs	250-295	1.6-2.0
	3 NZ EXs	1100	>3.9
GERESS	10 Vogtland EQs	140-260	1.4-3.2
	13 Vogtland QBs	165-210	2.0-2.6
	30 Lubin RBs	340-350	1.8-3.3
WMQ	23 EQs	100-1100	4.2-5.9
	16 Kazakh EXs	950	4.8-6.1
	1 Lop Nor EX	240	4.7
KNB	59 NTS EQs	295-310	2.1-5.9
	89 NTS EXs	280-315	2.4-5.5
MNV	37 NTS EQs	250-260	2.2-5.9
	78 NTS EXs	190-245	2.6-5.5

Discriminants considered in this study include Pn/Lg and Pn/Sn in 3-5, 4-6, 5-7, 6-8 Hz bands, and an Lg spectral ratio. Of these, only Pn/Lg in the 6-8 Hz band and Lg spectral ratio measurements were provided by LLNL for KNB and MNV. Also, Sn was measured for only 2 of 17 explosions recorded by WMQ. In the remainder of this section, we describe the discriminant data in more detail for each of the data sets at the various stations or arrays.

Baumgardt et al. (1992) describe how these discriminants are computed from seismic waveforms for the ARCESS, GERESS and WMQ data sets, while Walter et al. (1994) provide similar descriptions for the KNB and MNV data sets.

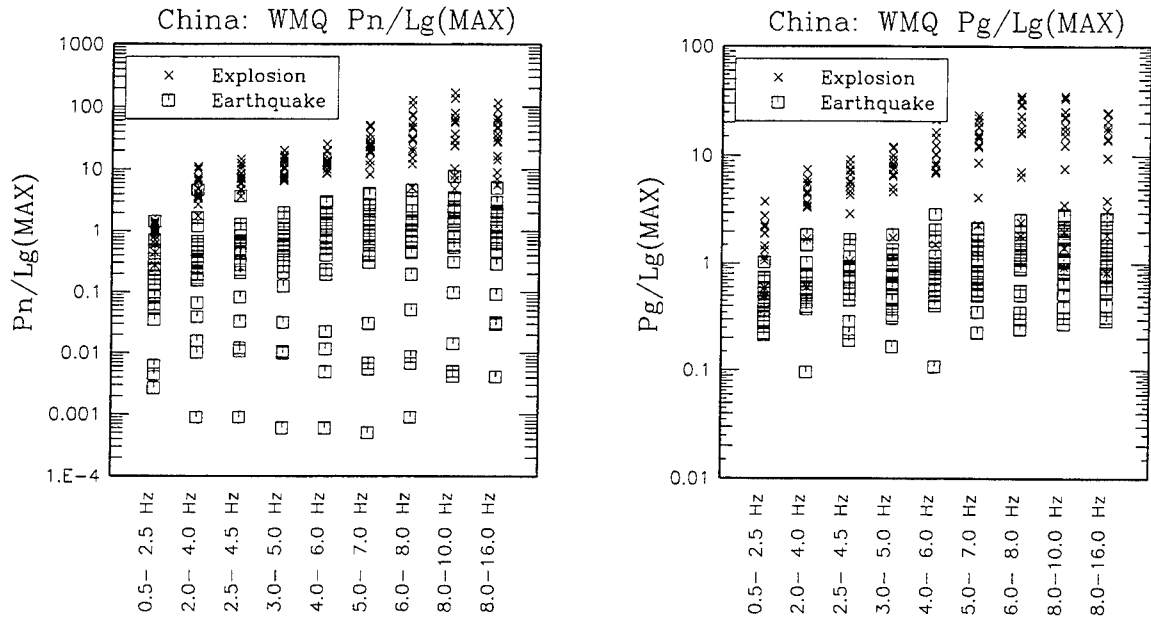
## 2.1. WMQ Data Set

Figure 2 shows locations of CDSN station WMQ, 16 nuclear explosions at the Balapan test site in Kazakhstan, the 29 September 1988 nuclear explosion at the Lop Nor test site in China, and 23 earthquakes scattered mostly around the northwest portion of China and western Mongolia. For WMQ, Pn/Lg and Pg/Lg measurements were made with the ISEIS system (Baumgardt and Der, 1994) on both the midband (bz) and high frequency (sz) vertical-component channels, with sampling rates of 20 and 40 Hz, respectively. In this study we focused on measurements of waveforms on the sz channel.



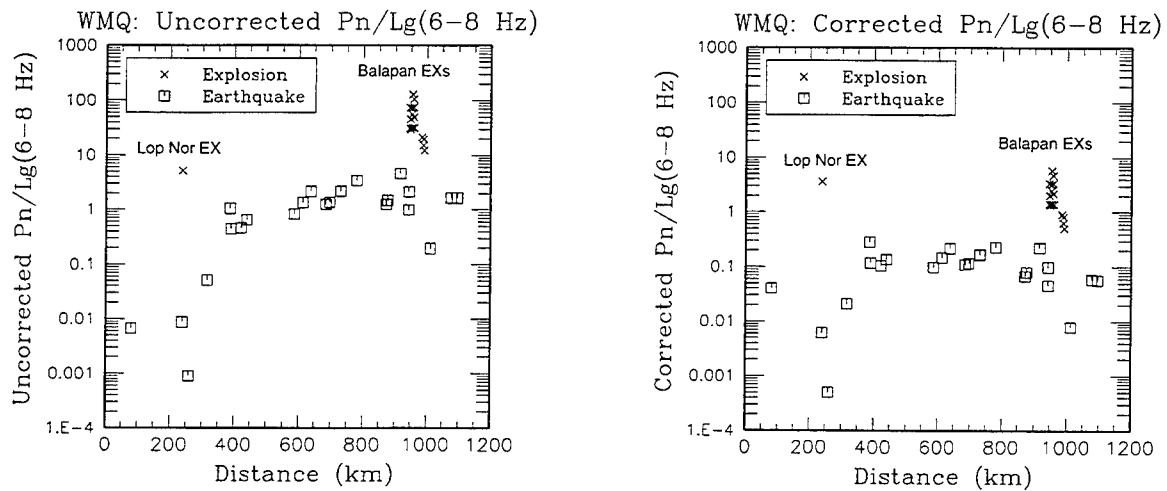
**Figure 2.** Locations of CDSN station WMQ, 16 nuclear explosions in Kazakhstan, the 880929 nuclear explosion at Lop Nor and 23 earthquakes in China and nearby countries.

Figure 3 shows Pn/Lg and Pg/Lg values (before applying distance corrections) for these events, based on maximum amplitude measurements in nine frequency bands ranging from 0.5 to 16 Hz. The mid-range frequency bands (3-8 Hz) provide the best separation of earthquakes and explosions. Since Lg attenuates more rapidly with distance than Pn and Pg in this region and the Lop Nor explosion is only 200 km from WMQ, it has the smallest Pn/Lg and Pg/Lg values of all the explosions and similar values in high frequency bands (6-16 Hz) to earthquakes at much greater distances.



**Figure 3.** Scatter plots of Pn/Lg (left) and Pg/Lg (right) in nine frequency bands, before applying distance corrections, for 17 nuclear explosions and 23 earthquakes recorded by station WMQ.

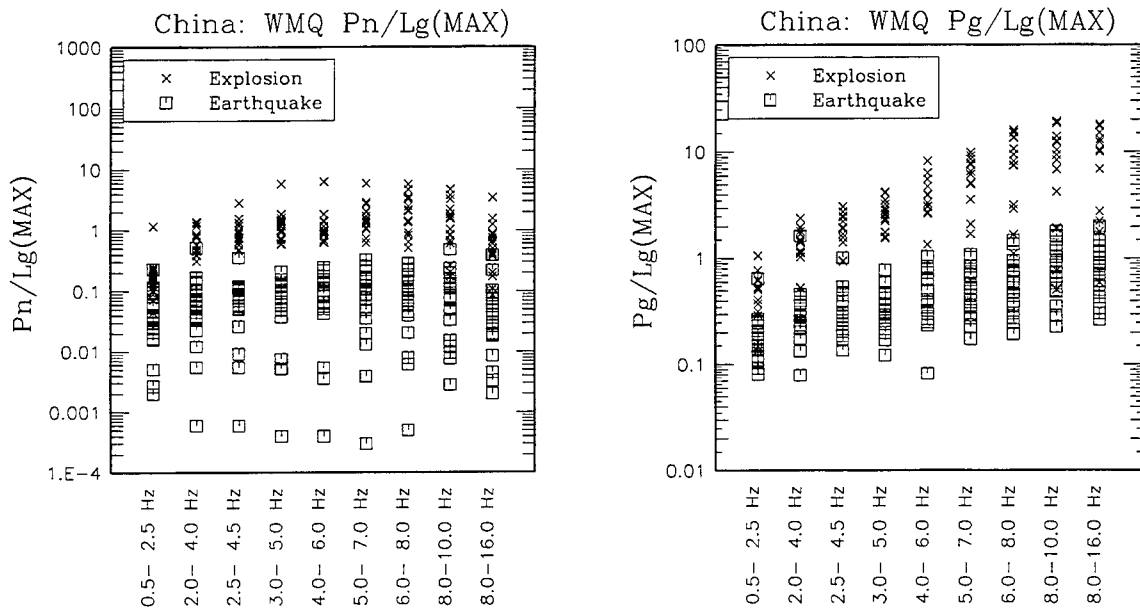
Figure 4 (left) shows the distance dependence of uncorrected Pn/Lg values in the 6-8 Hz band. Similar dependence is exhibited in the other frequency bands, as well as for Pg/Lg, although there are frequency and phase dependent variations. Note that the Lop Nor explosion at 200 km has the same uncorrected Pn/Lg(6-8 Hz) value as the earthquake with a distance to WMQ of roughly 900 km. Earthquakes with epicentral distances less than 300 km exhibit considerable scatter in their Pn/Lg and Pg/Lg values.



**Figure 4.** Plots of uncorrected (left) and distance-corrected (right) Pn/Lg values in the 6-8 Hz band versus epicentral distance for WMQ events.

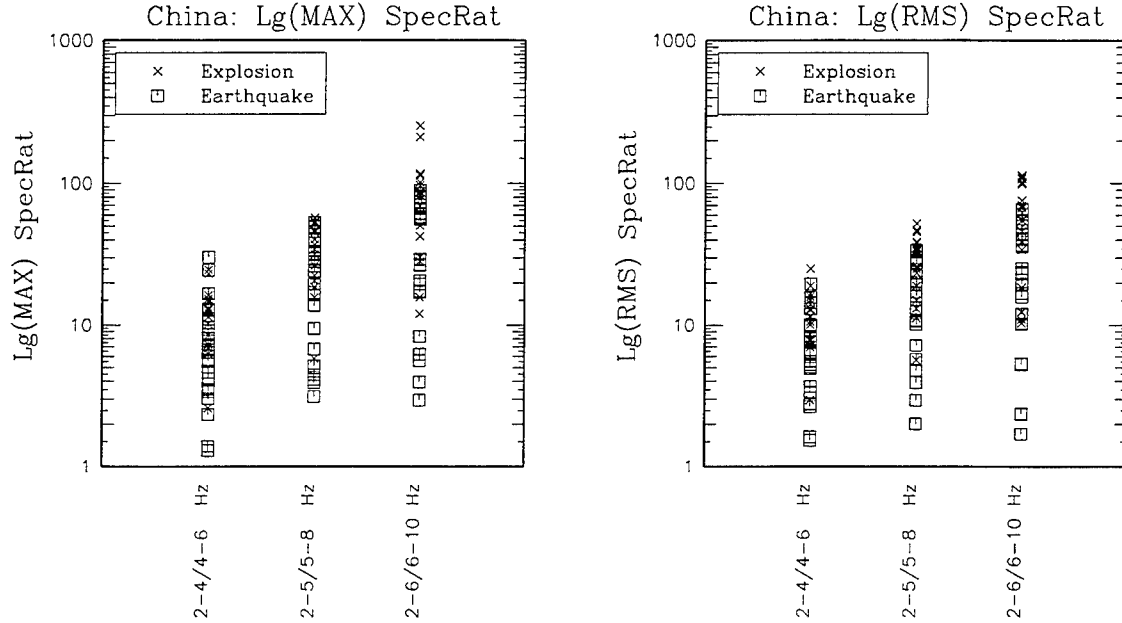
To remove this dependence, we derived and applied distance corrections to the amplitude ratios. To do this, we performed a least squares fit, using the earthquake data, and assuming a standard form of the relation of Pn/Lg to distance (e.g., Sereno, 1990):  $Pn/Lg(f)_{corrected} = (\Delta/\Delta_0)^{\alpha(f)} Pn/Lg(f)_{uncorrected}$ , where  $\Delta$  is the epicentral distance of the event,  $\Delta_0$  is a reference distance (taken to be 200 km), and  $\alpha(f)$  is a frequency dependent coefficient which is solved for in the least squares procedure. The problem is linearized with respect to  $\alpha(f)$  by taking the logarithm of both sides of this expression. Figure 4 (right) shows the distance-corrected Pn/Lg(6-8 Hz) values. The distance-corrected Pn/Lg and Pg/Lg values for the Lop Nor explosion are all now well within those for the Balapan nuclear explosions. There is still considerable scatter in Pn/Lg values for earthquakes at close distances. More events at these distances are desired to verify or improve the derived distance corrections.

Figure 5 shows scatter plots of the Pn/Lg and Pg/Lg values for the WMQ events after applying the derived distance corrections. Pn/Lg measurements in 3-5, 4-6, 5-7 and 6-8 Hz bands provide the best discrimination between explosions and earthquakes at WMQ. Pg/Lg measurements in 3-5, 4-6 and 5-7 Hz bands also separate explosions and earthquakes at WMQ. We did not, however, use Pg/Lg in the study presented below to assess regional identification performance since Pg/Lg does not discriminate as consistently in various regions as Pn/Lg and Pn/Sn. Also, Sn measurements were available for only 2 of the 17 explosions recorded by WMQ. Thus, we could not use Pn/Sn as a discriminant at WMQ.



**Figure 5. Scatter plots of Pn/Lg (left) and Pg/Lg (right) in nine frequency bands, after applying distance corrections, for 17 nuclear explosions and 23 earthquakes recorded by station WMQ.**

Figure 6 shows values of Lg spectral ratios for the WMQ events based on maximum (left) and rms (right) measurements of Lg spectra in three combinations of frequency bands. The plots show that Lg spectral ratios do not provide effective discrimination in this region.



**Figure 6.** Scatter plots of Lg spectral ratios for nuclear explosions and earthquakes recorded by WMQ, based on maximum (left) and rms (right) measurements of Lg spectra in three combinations of frequency bands on the sz channel.

## 2.2. ARCESS Data Set

ARCESS events used in this study include 24 earthquakes in the Steigen region of northern Norway, 5 earthquakes near Spitsbergen, 53 quarry blasts on the Kola Peninsula, 39 quarry blasts in the Kiruna region of Sweden, and 3 underground nuclear explosions at the Novaya Zemlya test site. Figure 7 shows the locations of these events and the ARCESS array. Table 1 summarizes their magnitudes and epicentral distances to the ARCESS array. We also analyzed an event which occurred on Novaya Zemlya on 31 December 1992 (921231). This event is labelled by its origin identification number (ORID = 361575) in Figure 7.

Figure 8 shows Pn/Lg values in nine frequency bands for the Kola Peninsula and Kiruna quarry blasts and Steigen earthquakes, before (left) and after (right) applying distance corrections. Pn/Lg measurements were not available for the 4 Novaya Zemlya events, nor the 5 earthquakes near Spitsbergen, since Lg does not propagate efficiently beneath the Barents Sea. Distance corrections used here were obtained from Sereno (1990) in which he derived distance relations for Pn, Pg, Lg and Sn in Fennoscandia based on 97 regional events recorded in common by ARCESS and NORESS. All events were reported in the



Helsinki Bulletin. (Distance corrections for Lg may be invalid for frequencies above 5 Hz due to attenuation of high-frequency Lg for events at far regional distances in this region. At present, however, these are the best corrections available.) Pn/Lg measurements in the 4-6 and 5-7 Hz bands provide the best discrimination of the Steigen earthquakes and Kola quarry blasts. Pn/Lg values for the Kiruna quarry blasts are more similar to those for the Steigen earthquakes before applying distance corrections, while more like those for the Kola quarry blasts after. (Cf. Table 1 for distances of these events to ARCESS.)

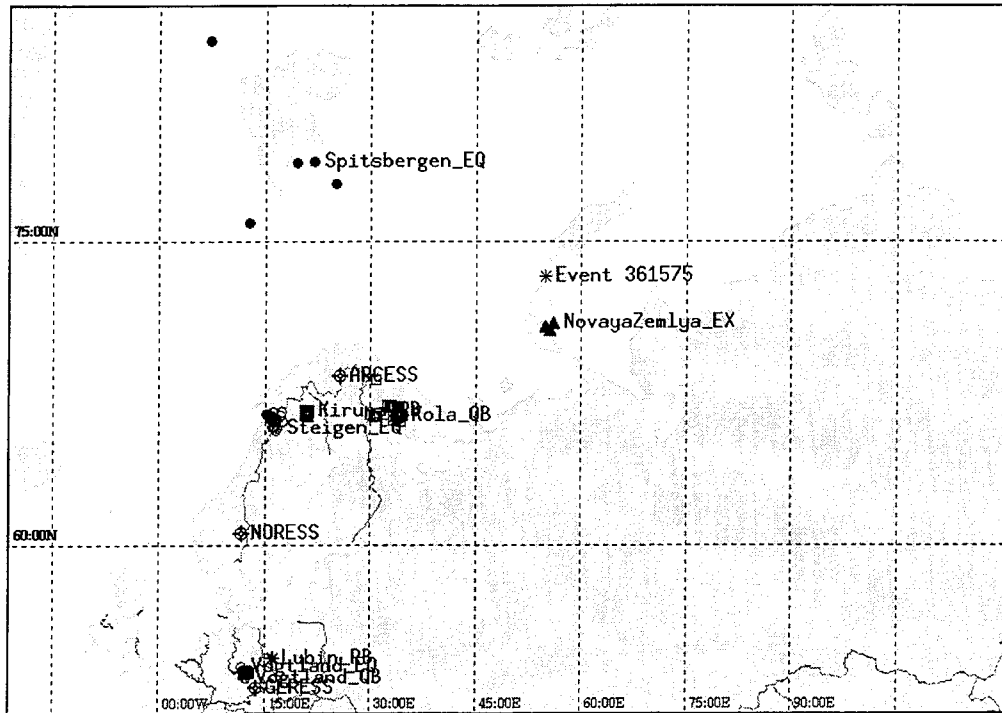


Figure 7. Locations of the ARCESS, GERESS and NORESS arrays and events used in this study.

Figure 9 shows scatter plots of Pn/Sn maximum amplitude measurements in six frequency bands, before (left) and after (right) applying distance corrections, for events recorded by the ARCESS array. These events include 53 Kola quarry blasts, 2 Kiruna quarry blasts, 24 Steigen earthquakes, 5 earthquakes near Spitsbergen, 3 nuclear explosions at the Novaya Zemlya test site, and the 921231 Novaya Zemlya event. The legends associate the marker type with the event type. Distance corrections for Pn/Sn were also obtained from Sereno (1990). Pn/Sn values were provided for only 2 of the 39 Kiruna quarry blasts.

There are several points to make regarding these data. First, Pn/Sn values for the Novaya Zemlya explosions are higher than those for the earthquakes, except in the 3-5 Hz band, for which Pn/Sn for an earthquake near Spitsbergen is greater than values in this band for all three nuclear explosions and most quarry blasts. Second, Pn/Sn does not discriminate

nuclear explosions from quarry blasts at ARCESS, particularly after applying distance corrections. Third,  $P_n/S_n$  values for the Steigen and Spitsbergen earthquakes are more consistent with one another after applying distance corrections. Fourth,  $P_n/S_n$  values for the 921231 event are more consistent with those for quarry blasts before distance-correcting, while more consistent with earthquakes after. Note, however, that the different frequency bands provide different evidence as to the identification of the 921231 event; its  $P_n/S_n(6-8 \text{ Hz})$  value seems peculiarly high as compared to other bands.

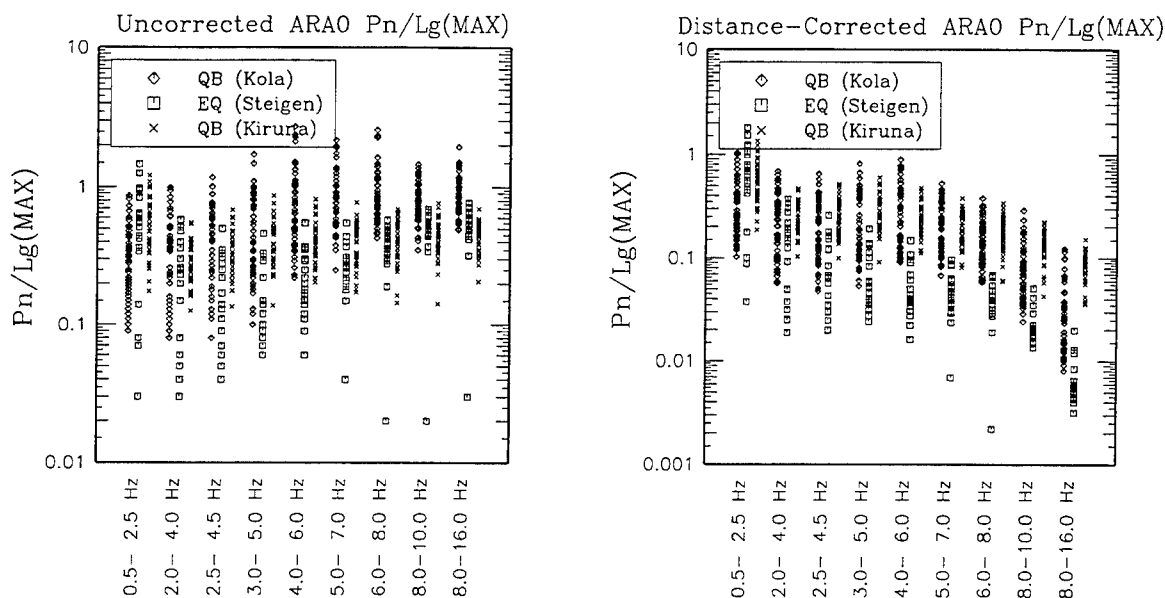


Figure 8. Scatter plots of  $P_n/L_g$  in nine frequency bands, before (left) and after (right) applying distance corrections, for 53 quarry blasts on the Kola Peninsula, 39 quarry blasts in the Kiruna region in Sweden and 24 earthquakes near Steigen, Norway, recorded by the ARCESS array.

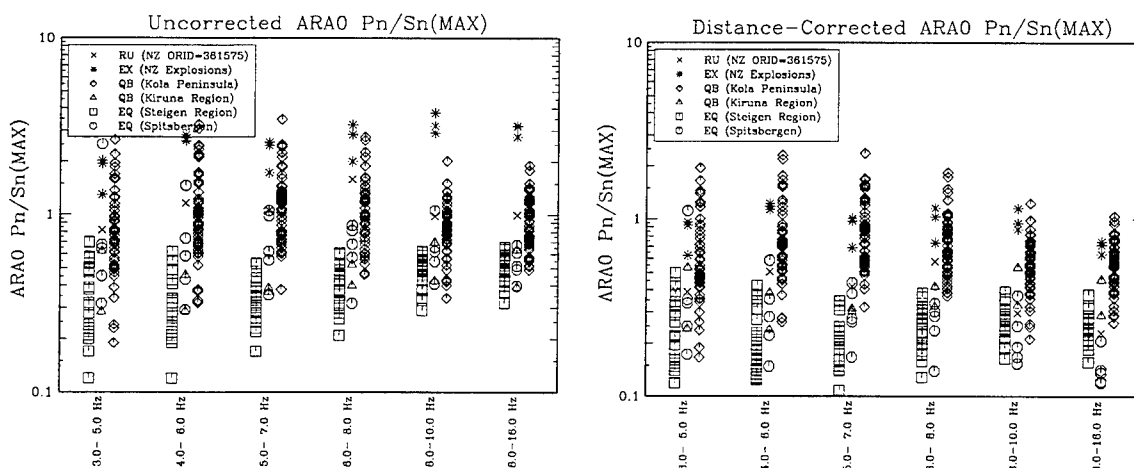
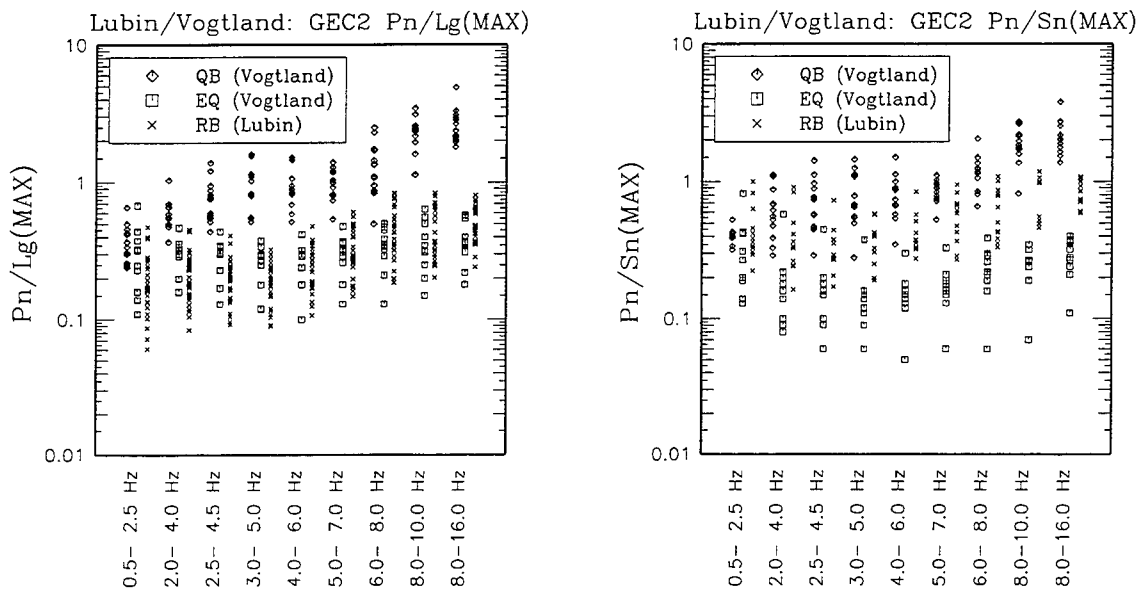


Figure 9. Scatter plots of  $P_n/S_n$  in six frequency bands, before (left) and after (right) applying distance corrections, for 53 Kola and 2 Kiruna quarry blasts, 24 Steigen and 5 Spitsbergen earthquakes, 3 Novaya Zemlya nuclear explosions, and the 921231 Novaya Zemlya event, recorded by ARCESS.

We were provided with Lg spectral ratios for the quarry blasts and one of the Steigen earthquakes, but none were available for the Novaya Zemlya, Spitsbergen, and remainder of the Steigen events. Thus, we were unable to use Lg spectral ratios for the ARCESS events in studies of regional identification performance.

### 2.3. GERESS Data Set

This data set includes 13 quarry blasts and 10 earthquakes which occurred in the Vogtland region, roughly 180 km northwest of the GERESS array. It also consists of 30 rock bursts or induced mine tremors in the Lubin Copper Basin in Poland, roughly 350 km northeast of GERESS. Figure 7 shows locations of these events relative to GERESS. (See Grant et al., 1993, for further details regarding these events.) Figure 10 shows Pn/Lg (left) and Pn/Sn (right) values in nine frequency bands, based on maximum amplitude measurements. (No distance corrections were applied to these data. However, the Vogtland quarry blasts and earthquakes are nearly collocated and their propagation distances are roughly equal to the reference distance,  $\Delta_0 = 200$  km, relative to which corrections are applied.)



**Figure 10. Scatter plots of Pn/Lg (left) and Pn/Sn (right) in nine frequency bands for 13 quarry blasts, 10 earthquakes and 30 rock bursts recorded by the GERESS array.**

The highest frequency bands provide the best discrimination of earthquakes and quarry blasts. Pn/Lg values for the Lubin rock bursts are very similar to those for the Vogtland earthquakes, while their Pn/Sn values fall between the values for the earthquakes and quarry blasts. This may be due to the fact that the rock bursts were shallow (less than 1 km deep), generating considerable Lg. Note that distance corrections would cause Pn/Lg and Pn/Sn values for the Lubin events to be even more like those for the Vogtland earthquakes.

Figure 11 shows Lg spectral ratios, based on maximum (left) and rms (right) measurements of Lg spectra in three combinations of frequency bands, for the Vogtland quarry blasts and earthquakes and Lubin rockbursts recorded by GERESS. Except for one quarry blast, the earthquakes and quarry blasts separate completely. Baumgardt et al. (1992) showed that this ripple-fired quarry blast generated large modulations in the observed spectrum, anomalously enriching the high frequency content. Lg spectral ratios for the Lubin rock bursts fall between the values for the earthquakes and quarry blasts. This is likely due to their shallow depth and near-source medium properties, as well as a mixture of source characteristics, since some of the tremors were induced by explosions (Baumgardt, 1994).

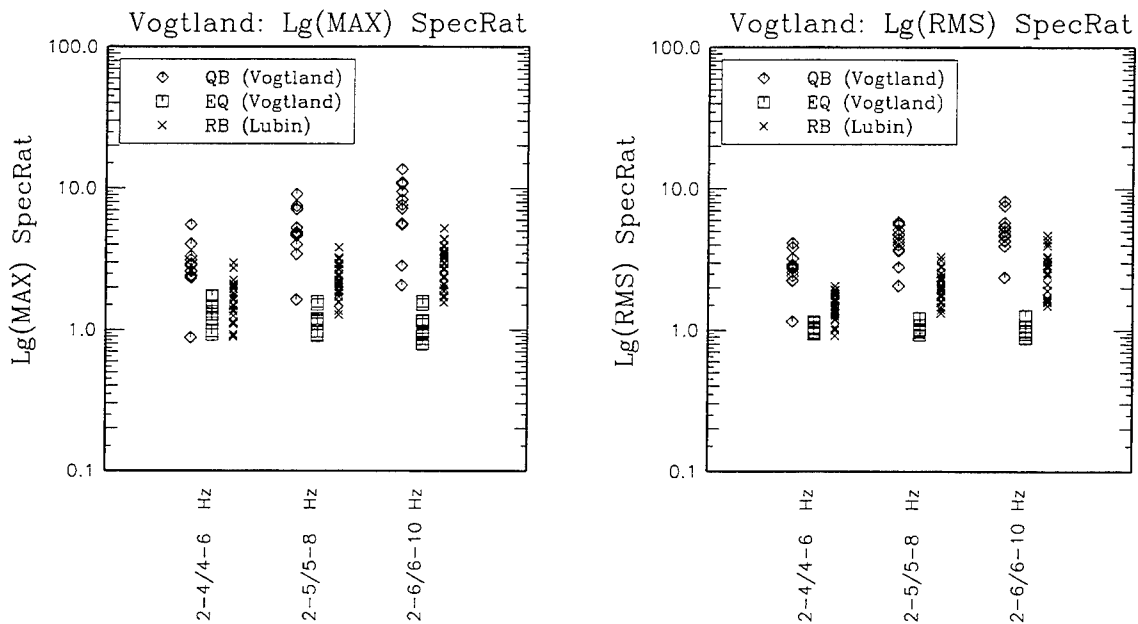


**Figure 11.** Lg spectral ratios for earthquakes, quarry blasts and rockbursts recorded by GERESS, based on maximum (left) and rms (right) measurements in three combinations of frequency bands.

#### 2.4. KNB and MNV Data Sets

Patton and Walter (1994) provided us with data for a total of 76 earthquakes, 141 nuclear explosions, and 1 contained 1 kt chemical explosion at NTS, recorded by LNN stations KNB and MNV. The chemical explosion was the September 1993 Non-Proliferation Experiment (NPE). Due to signal-to-noise limitations for some events, phase ratio and low-to-high spectral measurements were computed for 59 earthquakes and 89 explosions of the events recorded by KNB. Similar measurements were computed for 37 earthquakes and 78 explosions of those recorded by MNV. Measurements for the NPE were provided for both stations. Two other LNN stations, ELK and LAC, did not record many of these earthquakes due to intermittent operation during the period when they occurred (Walter et al., 1994).

Figure 12 shows a map of the southwestern U.S. depicting locations of LNN stations KNB and MNV relative to NTS. On the left of Figure 12 is an enlarged map of NTS showing epicenters of the nuclear explosions and earthquakes used in this study. The earthquakes, ranging from magnitude (ML) 2.1 to 5.9, were clustered in three main locations: Little Skull Mountain, Rock Valley, and one at Massachusetts Mountain. Walter et al. (1994) provide a detailed discussion of the mainshocks and aftershock sequences, their focal mechanisms, and a description of relevant geology. Most of the Little Skull Mountain sequence occurred between 6 to 12 km in depth (Meremonte et al., 1994), while the depth of the Rock Valley sequence was constrained to 1-3 km, based on measurements by a portable instrument located 1.5 km from the epicenter (Smith and Brune, 1993). The explosions ranged in magnitude from ML 2.4 to 5.5 and in depth from 200 to nearly 700 meters, in media with a relatively wide range of properties.

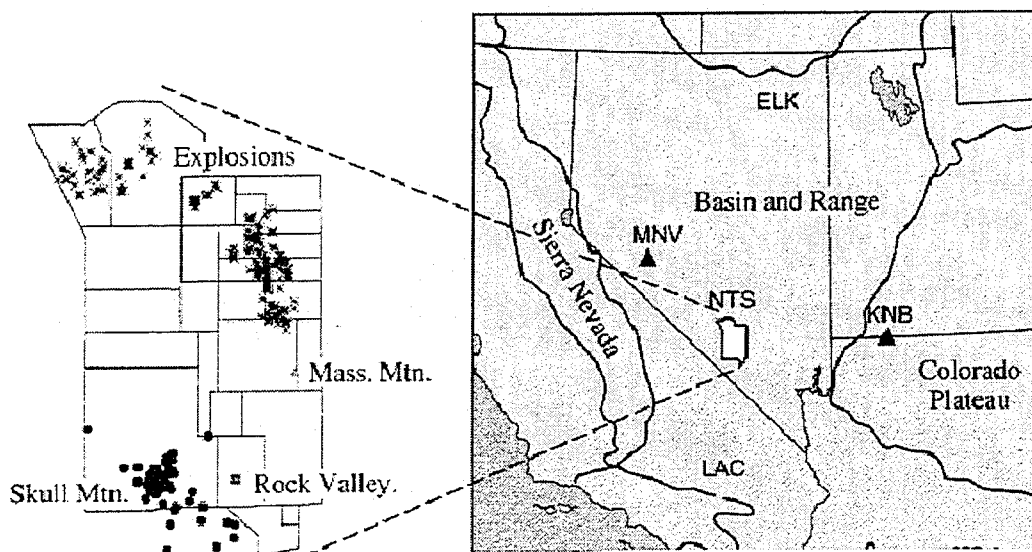


**Figure 12.** Map of the southwestern U.S. showing locations of LNN stations KNB and MNV relative to NTS. On the left is an enlarged map of NTS showing epicenters of the nuclear explosions and earthquakes used in this study. (Courtesy of W. Walter of LLNL.)

This data set has several interesting features with regard to assessing regional identification performance in the context of seismic monitoring of a CTBT. First, regional geology in the western U.S. complements that in the other regions considered in this study. Second, the events have similar paths, in contrast to previous western U.S. data sets (e.g., Taylor et al., 1989). Thus, source effects are better isolated from regional path variations. Third, there are earthquakes and nuclear explosions of widely varying magnitude, including explosions of magnitude 2.5 or less. Fourth, there are both shallow and normal-depth earthquakes. Fifth, there are nuclear explosions at various depths in media of varying properties; source medium properties such as density, P-wave velocity, and gas porosity are available for all

of the explosions. These features provide a unique data set with which to better understand effects of depth and source medium properties on regional discriminants.

Figure 13 shows Pn/Lg and Pg/Lg measurements in the 6-8 Hz band for the events recorded by KNB and MNV. (Note that Sn measurements were not available since Sn does not propagate efficiently in the western U.S.) The explosions are separated by those which were detonated in media with high versus low gas porosity (GP) and the earthquakes are separated into subregions in which they occurred. The legend associates the marker types with the various events. Pn/Lg values at MNV provide the best discrimination of earthquakes and explosions in this region, while Pg/Lg does not discriminate as well. There is more overlap of both Pn/Lg and Pg/Lg for the two event types at KNB than at MNV.

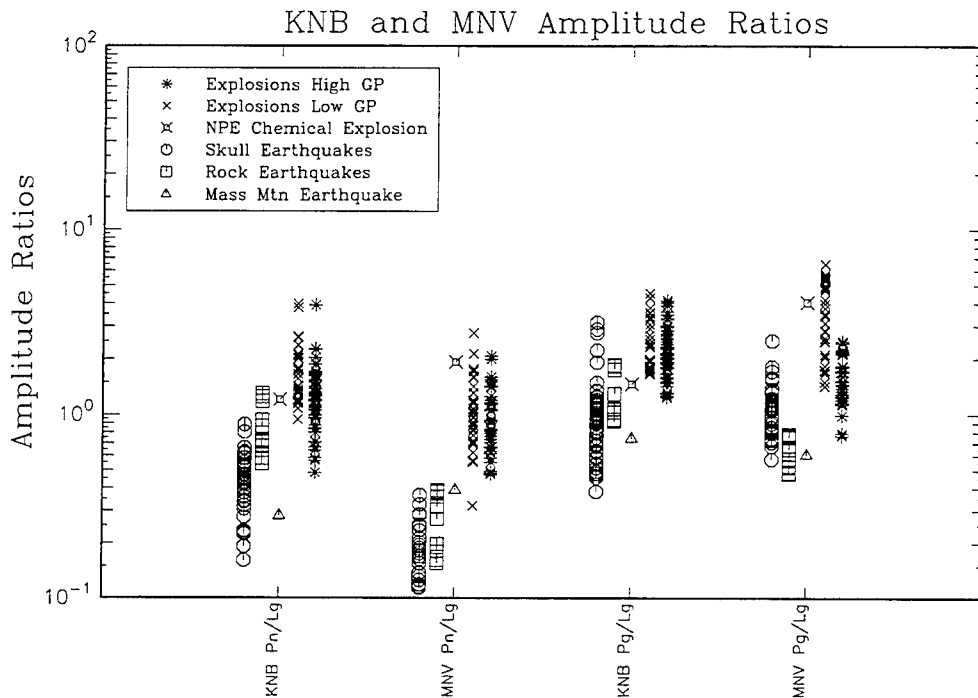
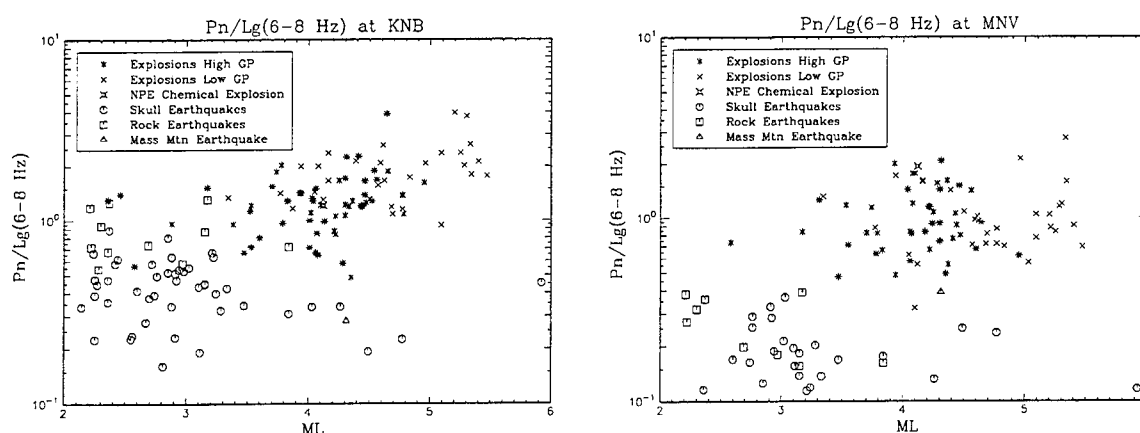


**Figure 13. Scatter plots of Pn/Lg and Pg/Lg measurements in the 6-8 Hz band for seismic events recorded by LNN stations KNB and MNV.**

Walter et al. (1994) noted that Pn/Lg and Pg/Lg exhibit differing values for shallow than for deeper earthquakes, with different dependence at the two stations and for the two types of phase ratios, possibly due to radiation pattern or path effects. There does not appear to be significant difference between Pn/Lg and Pg/Lg values for explosions in media of high versus low gas porosity, except for Pg/Lg at MNV for which explosions in media of high gas porosity typically have lower Pg/Lg values. By averaging P/Lg values over both stations, Walter et al. (1994) found that Pg/Lg values are generally lower for explosions in

high gas porosity media, while no such dependence was observed for Pn/Lg. Figure 14 shows that Pn/Lg in the 6-8 Hz band exhibits some dependence on magnitude, ML(coda), at MNV (right) and more noticeably at KNB (left), although this is actually a signal-to-noise effect. The same is also true of Pg/Lg.

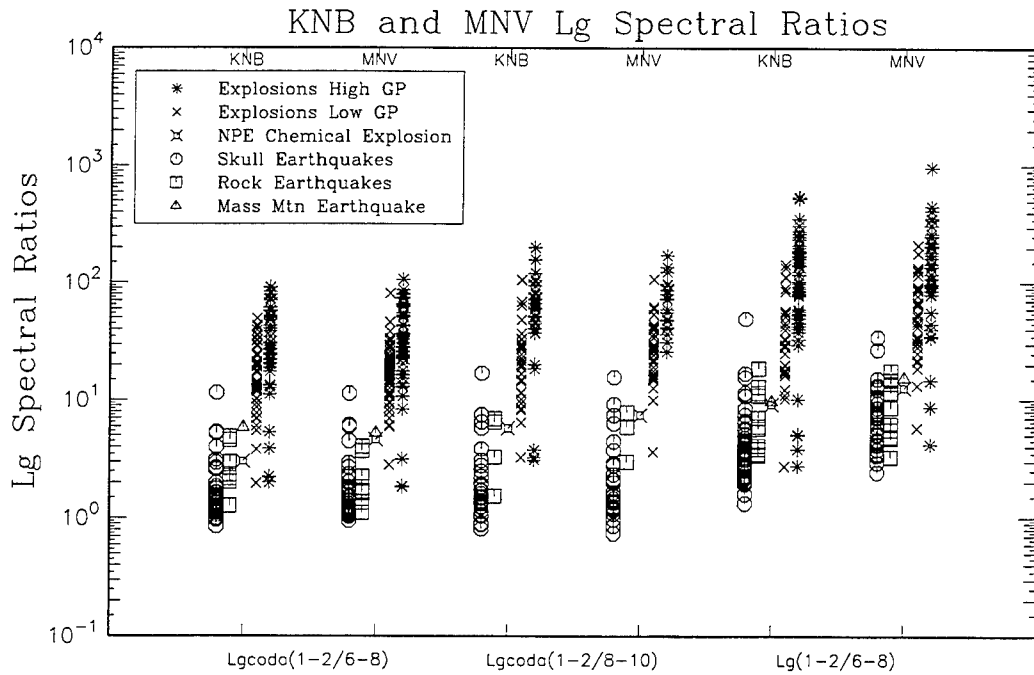
Note that the Pn/Lg and Pg/Lg values for the NPE are among the highest for explosions seen at MNV, while its Pn/Lg value at KNB falls in the middle of the explosion group and its Pg/Lg value at KNB is among the smallest. The cause of this differing behavior is not immediately apparent. However, it is clear that Pn/Lg and Pg/Lg do not discriminate nuclear and single contained chemical explosions in this region and, very likely, elsewhere.



**Figure 14. Pn/Lg measurements in the 6-8 Hz band versus ML(coda) for events recorded by KNB (left) and MNV (right).**

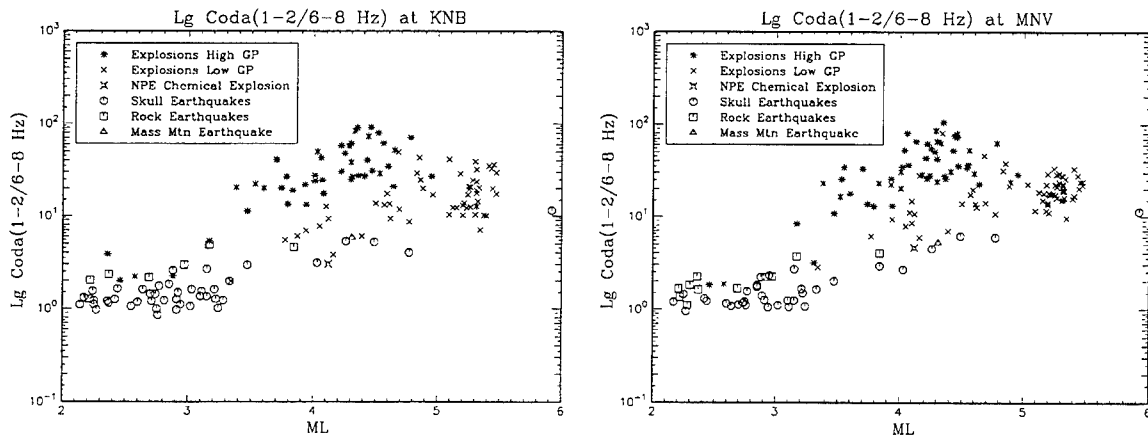
Note that discrimination using Pn/Lg(6-8 Hz) appears to be better at MNV than KNB for two reasons. First, Pn/Lg(6-8 Hz) measurements for the shallow Rock Valley earthquakes are noticeably high at KNB. Second, due to better signal-to-noise ratio (SNR) at KNB than MNV, there are measurements at KNB for more of the small events. Although these small events seen at KNB passed a SNR test, poorer SNR for small magnitude events contributes to more overlap of Pn/Lg values for earthquakes and explosions.

Figure 15 shows Lg spectral ratio values of three different types for the same events. The first two are ratios of Lg coda measurements in the 1-2 Hz versus 6-8 or 8-10 Hz bands. The third is the ratio of direct Lg measurements in the 1-2 Hz versus 6-8 Hz bands. Of these, Lgcoda(1-2 Hz/8-10 Hz) at MNV discriminates the best although, due to poorer SNR in the 8-10 Hz band, Lgcoda(1-2 Hz/6-8 Hz) was measured for more events and provides nearly as effective discrimination. Thus, Lgcoda(1-2 Hz/6-8 Hz) was used, along with Pn/Lg(6-8 Hz) in the identification studies described in Section 4.



**Figure 15.** Scatter plots of Lg spectral ratio measurements of three different types for seismic events recorded by LNN stations KNB and MNV. Events are separated into subgroups as in Figure 13.

Figure 16 shows that Lg spectral ratios exhibit significant magnitude dependence. In fact, Walter et al. (1994) noted that none of the spectral ratios discriminate well for events below ML 3.5. For explosions, they also showed that Pn, Pg and Lg spectral ratios exhibit strong dependence on gas porosity of the near-source medium, as a function of magnitude, and not explicitly on event depth.



**Figure 16.** Spectral ratio (1-2 Hz/6-8 Hz) measurements of Lg coda versus ML(coda) for events recorded by KNB (left) and MNV (right). Lg spectral ratios exhibit significant magnitude dependence and do not discriminate earthquakes and explosions in this region below ML 3.5.



In summary,  $Pn/Lg(6-8\text{ Hz})$  provides the best discrimination, particularly at MNV, and varies some, but not dramatically, with magnitude or source medium properties.  $Pn/Lg$  does exhibit some dependence on source depth for earthquakes seen at KNB, with higher values for shallower earthquakes, making them more difficult to discriminate from explosions there. This may be due, at least partially, to radiation pattern or path effects.  $Pg/Lg$  does not discriminate as well as  $Pn/Lg$  and appears to be more sensitive to near-source and path effects.  $Pg/Lg$  does not vary dramatically with magnitude, nor consistently with depth or source medium properties from one station to the other.  $Pg/Lg$  at MNV or station-averaged does, however, exhibit correlation to gas porosity for the explosions.  $Lg$  spectral ratios provide fairly good discrimination for events above ML 3.5, particularly for high gas porosity explosions.  $Lg$  spectral ratios do exhibit strong correlation to magnitude, as well as to gas porosity, with no significant correlation explicitly to depth.

## **2.5. Data Set Comparisons and $Pn/Lg$ Transportability**

Comparisons of high-frequency discriminants for the different regions represented by the various data sets in this study are interesting from the standpoint of understanding where certain discriminants work and effects of regional tectonic variations. First,  $Lg$  spectral ratios appear to discriminate at GERESS and in the western U.S., but not at WMQ or ARCESS. Second, high-frequency  $Pg/Lg$  discriminates fairly well at WMQ, GERESS and in the western U.S., but not at ARCESS. Third, high-frequency  $Pn/Lg$  and  $Pn/Sn$  appear to discriminate robustly in most regions for which  $Lg$  or  $Sn$  are observed. In many cases both  $Pn/Lg$  and  $Pn/Sn$  can be measured and used, while in others either  $Sn$  or  $Lg$  is attenuated or blocked by regional structures.  $P/Sn$  does not appear to be a viable discriminant at WMQ and in the western U.S. since  $Sn$  signals are too weak in these regions, particularly for explosions.  $P/Lg$  does not appear to be useful for events with paths beneath oceans nor for paths with thin crustal structure (e.g., Baumgardt, 1990). These observations are consistent with those of Bennett et al. (1989), Baumgardt et al. (1992) and many others.

It has long been recognized that different seismic phases attenuate at different rates as functions of distance and frequency, even for relatively simple earth structures. In general,  $Sn$  and  $Lg$  attenuate more rapidly with distance than  $Pn$  or  $Pg$ . Thus, events at far regional distances may appear to be more explosion-like than ones at closer distances. This allows for the possibility that nearby explosions or distant earthquakes may be misidentified. An example is the identification of a 921231 Novaya Zemlya event, roughly 1100 km from ARCESS. Before applying distance corrections to the  $Pn/Sn$  discriminants, Baumgardt (1993b), Fisk and Gray (1993) and Pulli and Dysart (1993) found this event to be far more

consistent with quarry blasts on the Kola Peninsula than earthquakes in Scandinavia, whose distances ranged from 300 to 500 km. (All authors agreed that this event was not a nuclear detonation.) These results are inconsistent with a statement by the Russian Federation that no blasting had occurred. After applying distance corrections, Fisk (1993) found that this event was rejected as a quarry blast. In addition, Figure 4 illustrates how the 880929 Lop Nor nuclear explosion recorded by WMQ could be misidentified using uncorrected Pn/Lg values. Thus, distance-correcting Pn/Lg and Pn/Sn is very important.

Also, the optimal frequency band for Pn/Lg and Pn/Sn depends on the characteristics of the seismic instruments and filter functions used, as well as on regional geophysical effects. For example, Pn/Lg and Pn/Sn at 4-7 Hz discriminate the best at ARCESS, while those at 8-16 Hz discriminate much better at GERESS. In general, Pn/Lg and Pn/Sn in the 3-8 Hz band appears to discriminate the most consistently in all regions we have studied.

Although these discriminants typically separate earthquake and explosion groups, the threshold between the two groups can vary dramatically in different regions. Figure 17, for example, shows plots of uncorrected (left) and distance-corrected (right) Pn/Lg in the 6-8 Hz band for the various events recorded by ARCESS, GERESS, WMQ, MNV, and KNB. The discrimination threshold for uncorrected Pn/Lg at WMQ is roughly a factor of ten greater than those at the other stations. The distance-corrected thresholds are all fairly similar except for the threshold at ARCESS, which differs by almost an order of magnitude. (Note that the distance corrections for Pn/Lg at ARCESS may be invalid for this frequency band, although these were the best corrections available.) Even for the distance-corrected case, a threshold obtained for KNB would lead to missed nuclear explosions at WMQ. Similarly, the threshold for WMQ would lead to roughly a 30% false alarm rate at KNB. Since, in most cases, there is no clean separation between the earthquake and explosion groups, the threshold must be set very precisely in order to have high identification and low false alarm rates. Thus, a discrimination rule established in one region does not readily apply to another. (Note that the outlier-detection approach we use in Section 4 does not rely on transporting discrimination thresholds.)

Relative path corrections may improve Pn/Lg transportability. Progress has been made by Baumgardt and Der (1994) and Lay and Zhang (1994) in relating Pn/Lg values to tectonic (crustal and topographic) properties, although there are non-negligible uncertainties. Evidence suggests that empirical path corrections and theoretical modeling must be very accurate to succeed. Station corrections may also be needed. Note that many of the same

events were observed at MNV and KNB, while the Pn/Lg discrimination thresholds differ somewhat for the two stations. Practical difficulties include the fact that a common set of regional events, needed to derive corrections for a station lacking nuclear explosion data, is unlikely to also be recorded at stations for which such data exist. As a result of these complications, it has yet to be shown that a regional high-frequency discrimination threshold from one region can be successfully used to identify events in a new region.

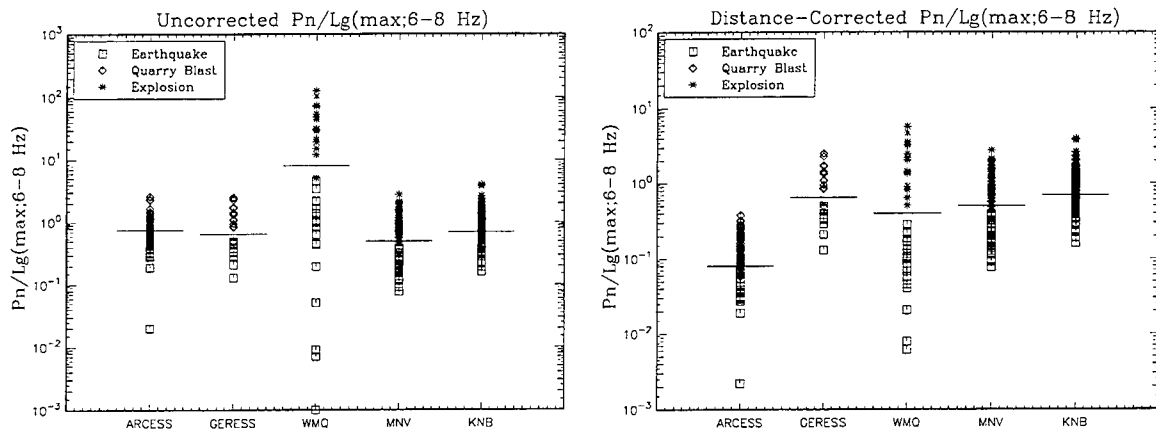


Figure 17. Uncorrected (left) and distance-corrected (right) Pn/Lg(6-8 Hz) for events recorded by ARCESS, GERESS, WMQ, MNV and KNB. Horizontal lines depict discrimination thresholds for each station.

### 3. Technical Approach

#### 3.1. Motivation

The objective is to identify underground nuclear explosions down to a few kilotons (kt) or less, possibly as low as 1 kt decoupled. A 1 kt decoupled explosion corresponds roughly to a magnitude 2.5 event or, equivalently, the size of a relatively large mining blast (Blandford et al., 1992). Above this threshold, Ringdal (1984) and Lilwall and Douglas (1985) estimate that there will be roughly 200,000 earthquakes worldwide per year. In addition, there will be a large number of quarry blasts and induced mine tremors that occur annually worldwide, although there is some debate as to explicit numbers. Nevertheless, it is clear that there will be many thousands of competing seismic signals, mostly from earthquakes and mining blasts, from which to try to identify a potential underground nuclear test.

Our goal is to provide an automated procedure to flag suspicious event which warrant special attention so that they can be investigated further by expert analysts and, possibly, by non-seismic techniques (e.g., on-site inspection). Unfortunately we lack seismic calibration data for nuclear explosions in most regions around the world. In addition, as

discussed above in Section 2.5, it has yet to be shown that a regional high-frequency discrimination threshold from one region can be successfully transported in order to identify events in a new region. Thus, in most cases, event identification, within the context of CTBT or NPT monitoring, is a problem of detecting unusual events, i.e., outliers.

For regions in which training information is available for more than one class of events (e.g., for regions which include historical test sites) we also developed a classification test, based on the same methodology as the outlier test. This test provides improved identification accuracy over the outlier test for cases in which more information is available. Below we primarily concentrate on monitoring results obtained using the outlier test because of its more general applicability.

### **3.2. Outlier Detection Approach**

If a station exists or has been recently installed, the first step is to collect a set of events recorded by the station. In most practical situations, we will not know the event types, a priori. An assumption is made that the number of new nuclear tests in a region will be relatively small compared to the number of earthquakes, mining blasts or rock bursts. If this assumption fails, i.e., if a region is aseismic and with no mining activity, then any new event would be suspicious, warranting further investigation. Since there are only a small number of mining blasts that occur annually above mb 3, our primary concern for monitoring above this threshold is to distinguish nuclear explosions from earthquakes. We focus on this case first. (Monitoring down to magnitude 2.5 poses greater difficulty.) In Section 4.2, we also consider the case in which earthquake data sets are contaminated by large quarry blasts or rock bursts and assess how this impacts monitoring performance.

A standard set of discriminants is used, unless we know that particular ones work best for a given region. In this study we use Pn/Lg and Pn/Sn in the 3-5, 4-6, 5-7 and 6-8 Hz bands, as well as an Lg spectral ratio, provided measurements were available for the events. In general, the outlier test can rigorously include any discrete or continuous discriminant from single or multiple stations and arrays. Distance corrections are applied if information is available. Each event is then tested as an outlier of the remaining data set using a hypothesis test based on the generalized likelihood ratio. (Technical details of the outlier test and previous applications are provided by Baek et al., 1992; Fisk et al., 1993a, 1993b; Fisk and Gray, 1993; Fisk, 1993.) Events flagged as outliers can be investigated further using, possibly, non-seismic means. The significance level of the test is an input parameter which controls the false alarm rate, e.g., the percentage of earthquakes flagged as outliers.

The basic idea behind the likelihood ratio test is to form the ratio of likelihoods,

$$\lambda = \frac{\max L(\text{parameters} \mid \text{data}; \text{under null hypothesis})}{\max L(\text{parameters} \mid \text{data}; \text{under alternative hypothesis})}, \quad (1)$$

where the numerator is computed under the null hypothesis being tested, given the data, and the denominator is computed under the alternative hypothesis. For the outlier test, the null hypothesis is that the event being tested belongs to the same population as the remainder of the events. The alternative hypothesis is that it does not. Since the true parameters of the likelihood functions are unknown, maximum likelihood estimates (MLEs) are computed from the data, subject to the particular hypothesis, and inserted into the likelihood functions. This yields the ratio of maximized likelihoods. The MLEs of the unknown parameters (e.g., the mean and covariance matrix of the discriminants) are computed subject to these two hypotheses.

Small values of  $\lambda$  indicate that the null hypothesis should be rejected. To quantify what is meant by “small”, the distribution of  $\lambda$  is needed. In general, its distribution is quite complicated, depending on the multivariate distribution of the the discriminants. To estimate it empirically, we use the bootstrap technique (Efron, 1979) to generate random samples from the distribution of actual data. Bootstrapped data is inserted in the likelihood ratio for many samples to obtain its distribution. From this distribution, the critical value is set so that the test has a specified false alarm rate. All events whose likelihood ratio are less than the critical value are considered outliers at the specified significance level.

The key innovation of our approach is the combination of the likelihood ratio and bootstrap techniques, which allows application to any discriminant distribution for which the MLEs exist, while controlling the error rate associated with a particular type of event. In addition, the likelihood ratio is a useful metric with which to rank events, by combining multivariate discriminant data in a univariate expression. (This capability is illustrated in Section 4.) This provides an alternative to imposing a rigid “yes/no” judgement and a means to focus on the most “suspicious” events.

### 3.3. Classification Approach

For regions in which training data are available for two or more types of events (e.g., for any combination of two or more training sets in a region which include earthquakes, quarry blasts, rock bursts or nuclear explosions), we developed a classification test, based also on

the likelihood ratio methodology (e.g., Baek et al., 1993; Fisk et al., 1993a). In this case the likelihood functions are extended to treat training data for two event classes and the event in question is allocated into one of two classes. (The test is applied sequentially to cases with more than two training sets. Future work is planned to extend the methodology to explicitly treat more than two event classes.) This method provides a hypothesis test in which one of the error rates is controlled or a classification test in the conventional sense in which the overall error rate or a cost function is minimized. Like the outlier test, it also allows events to be ranked straightforwardly. Fisk et al. (1993a) showed that this test has greater accuracy than the outlier test if more information is available.

The explicit form of the outlier and classification tests depend on the distributions of the discriminants used which, in general, may differ for different sets of discriminants and event types. Thus, we have implemented statistical algorithms to test appropriate assumptions and, if necessary, to transform the data to a form which ensures validity. Also, in many cases some of the discriminant values are missing for particular events. This may be due, for example, to blockage or strong attenuation of particular seismic phases, poor signal-to-noise, interference by other events, or instrument malfunction. Gray et al. (1994) generalized the methods to treat missing discriminant measurements for some of the events. We have also implemented an algorithm to automatically select the best set of discriminants for a given region if adequate training sets are available.

## **4. Monitoring Applications**

### **4.1. Applications of the Outlier Test**

Using the procedure described in Section 3.2, we sequentially used each of the nuclear explosions in each region as the “new” explosion. Each explosion was tested against the earthquakes to determine the percentage identified as outliers. We also considered each of the quarry blasts as the “new” explosion in their respective regions to supplement the nuclear explosion data. (Note that it is generally more difficult to discriminate earthquakes from quarry blasts than contained nuclear explosions. Thus, if quarry blasts are detected as outliers of the earthquake group, a nuclear explosion is also very likely to be detected.) Each earthquake was also sequentially tested using the leave-one-out procedure to estimate the false alarm rate. In the following, we set the significance level at 0.01 which, in practice, should lead to a false alarm rate of 1%. Doing this, we obtained the following results.

For ARCESS, using the Steigen and Spitsbergen earthquakes to train the outlier test, 3 of 3 Novaya Zemlya nuclear explosions, 50 of 51 (98%) Kola quarry blasts, and 36 of 39 (92%) Kiruna quarry blasts were flagged as outliers once distance corrections were applied to the discriminants. For GERESS, using the Vogtland earthquakes to train the outlier test, 13 of 13 Vogtland quarry blasts were detected as outliers. There were no false alarms at either ARCESS or GERESS. For CDSN station WMQ, 17 of 17 Balapan and Lop Nor nuclear explosions were flagged as outliers with 1 false alarm out of 23 earthquakes. For the LNN stations, 74 of 78 (95%) and 71 of 89 (80%) NTS nuclear explosions were detected as outliers at MNV and KNB, respectively, with one false alarm at each station.

These results show that useful monitoring can be performed with the outlier-detection approach, currently down to magnitude 3, for regions that are well-covered by at least one seismic station or array. Between 92–100% of the explosions and quarry blasts were detected as outliers of the earthquake groups in the various regions, except at KNB where the detection rate was 80%. There was one false alarm at each of the stations KNB, MNV and WMQ. Overall, 264 of 290 (91%) explosions were detected and there were only 3 false alarms out of 158 earthquakes (1.9%), slightly higher than the target rate of 1%. Figure 18 summarizes these results, which were obtained for diverse geological regions, seismic stations and arrays, and for a wide range of epicentral distances and magnitudes.

### Outlier Detection and False Alarm Rates

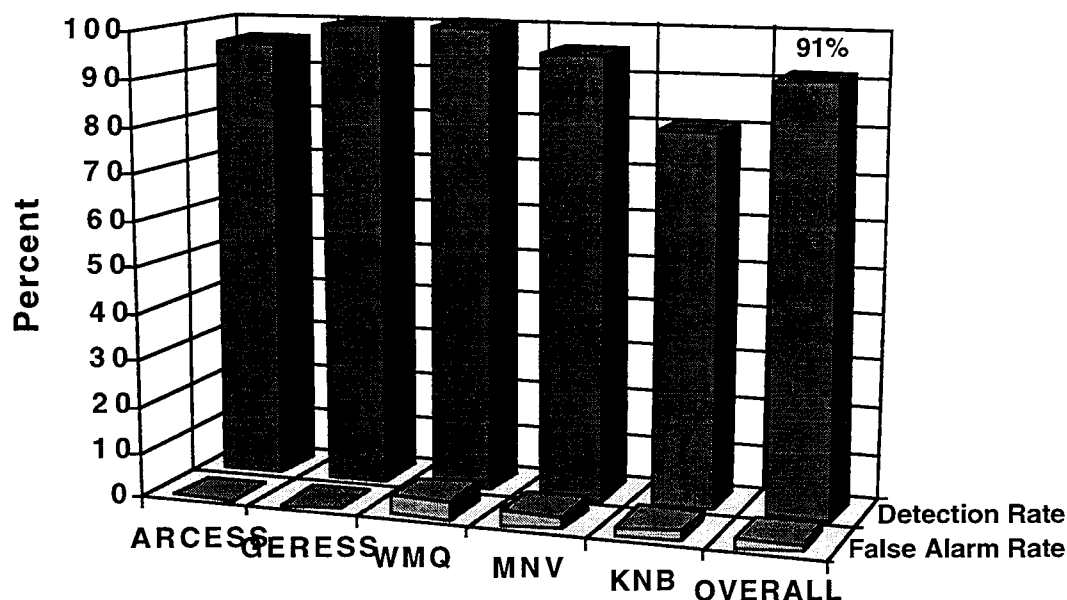
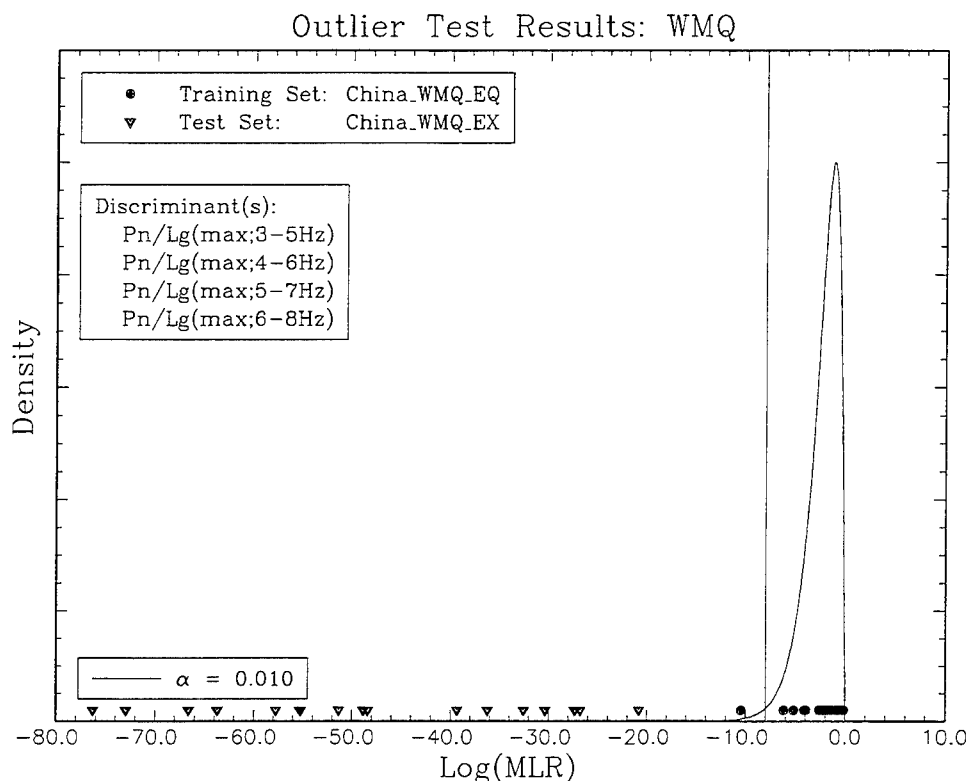


Figure 18. Summary of outlier test results (detection and false alarm rates) at ARCESS, GERESS, WMQ, MNV and KNB. Overall results are shown on the far right.

Results of the outlier tests for the various stations are illustrated in Figures 19–22. Figure 19 shows outlier test results for the events observed at WMQ. The distribution shown is of the likelihood ratio when the event being tested is from the same group as the earthquake training set, i.e., when the null hypothesis is true. The vertical line represents the threshold of the test for the significance level listed in the lowest legend. Events whose likelihood ratios are less than the threshold are identified as outliers at the corresponding significance level. The triangles and circles depict values of the likelihood ratio for the explosions and earthquakes being individually tested, respectively. The middle legend lists the discriminants used. (Recall that Pn/Sn was not available for most of the WMQ explosions.)



**Figure 19. Graphical representation of outlier test results for the WMQ events. The triangles and circles show values of the likelihood ratio for the explosions and earthquakes being tested, respectively. Event whose likelihood ratios are less than the threshold (vertical line) are identified as outliers.**

Figure 19 shows that all 17 nuclear explosions are flagged as outliers of the earthquake group at 0.01 significance level. Figure 19 also illustrates how the likelihood ratio combines multivariate data (e.g., values of five different discriminants in this case) into a single variable which allows events to be ranked in a statistically consistent manner, rather than providing a “yes/no” decision. Events with the smallest likelihood ratios (out in the tail) would be considered the most suspicious and could be investigated first.



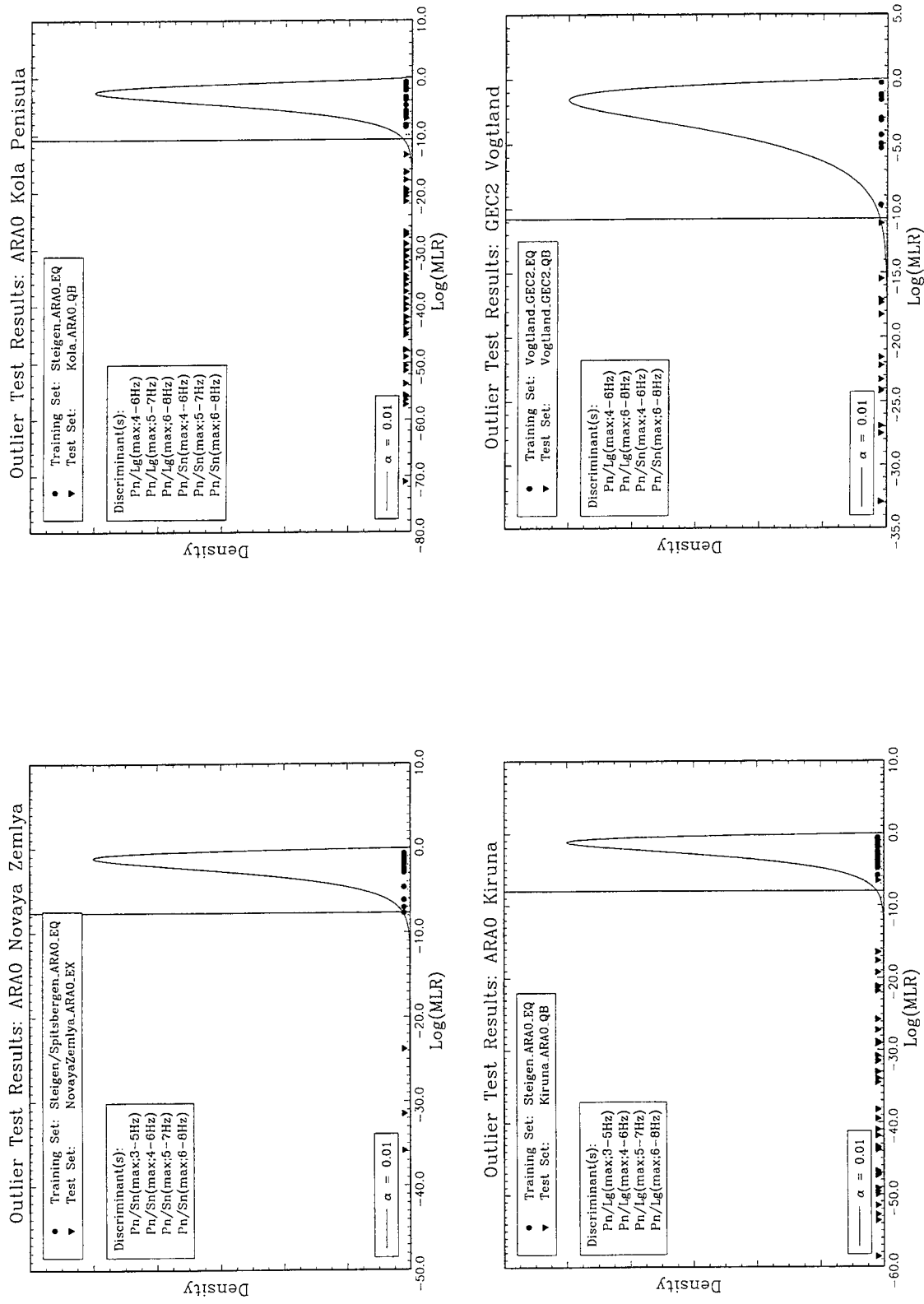
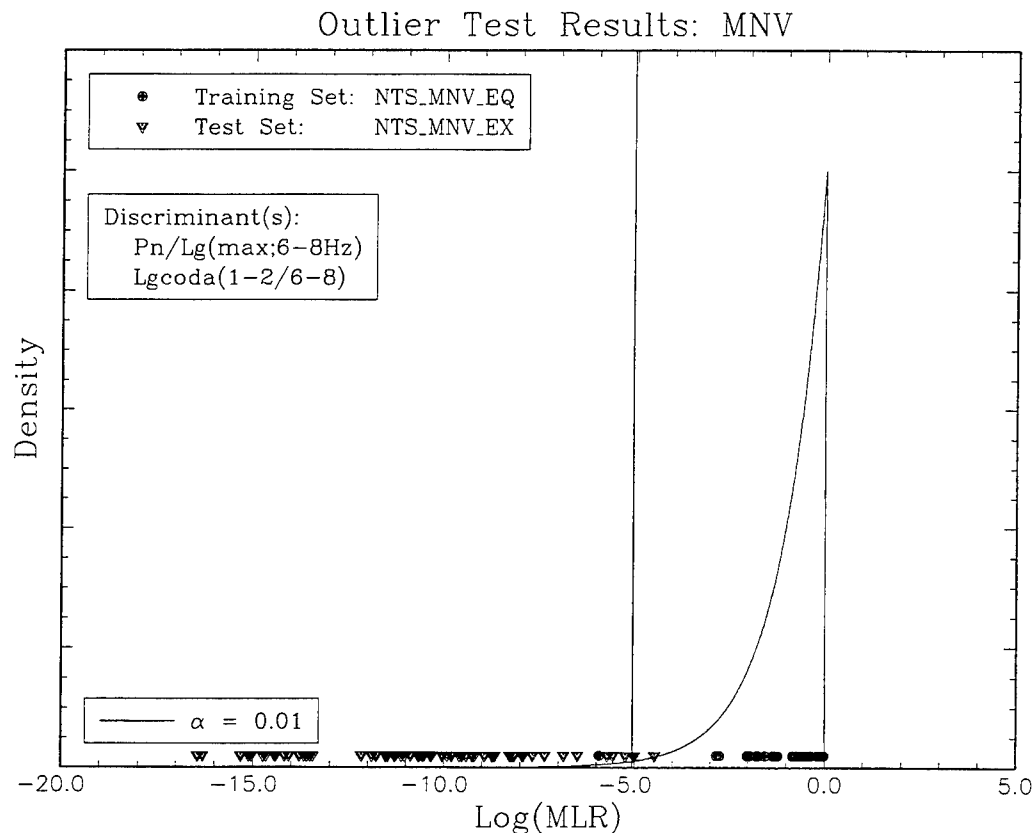


Figure 20. Graphical representations of outlier test results for Novaya Zemlya nuclear explosions (upper left), Kola quarry blasts (upper right), Kiruna quarry blasts (lower left), and Vogtland quarry blasts (lower right). The triangles depict values of the likelihood ratio for the explosions while the circles correspond to values of the likelihood ratio for the earthquakes considered at each array.

Figure 20 shows similar results of outlier tests performed on events recorded by ARCESS and GERESS. The upper left plot shows that all three of the Novaya Zemlya nuclear explosions recorded by ARCESS were detected as outliers at 0.01 significance level. The Steigen and Spitsbergen earthquakes were used as training data in this case. Likewise, the upper right plot shows results for the Kola quarry blasts seen at ARCESS. The five Spitsbergen earthquakes were not used in this case to make use of Pn/Lg which was measured for the Kola and Steigen events. The lower left plot shows that 36 of the 39 Kiruna quarry blasts recorded by ARCESS were detected as outliers. The lower right plot shows that all 13 of the Vogtland quarry blasts recorded by GERESS were identified as outliers. There were no false alarms for any of these cases.

Figure 21 shows results of outlier tests performed on events recorded by MNV. In this case, 74 of 78 nuclear explosions were detected as outliers at 0.01 significance level and there was 1 false alarm out of 37 earthquakes. Last, Figure 22 shows results of outlier tests performed on events recorded by KNB. In this case, 71 of 89 nuclear explosions were detected as outliers and there was 1 false alarm out of 59 earthquakes.



**Figure 21. Outlier test results for MNV events with both discriminant values present. The triangles and circles show values of the likelihood ratio for the explosions and earthquakes being tested, respectively.**

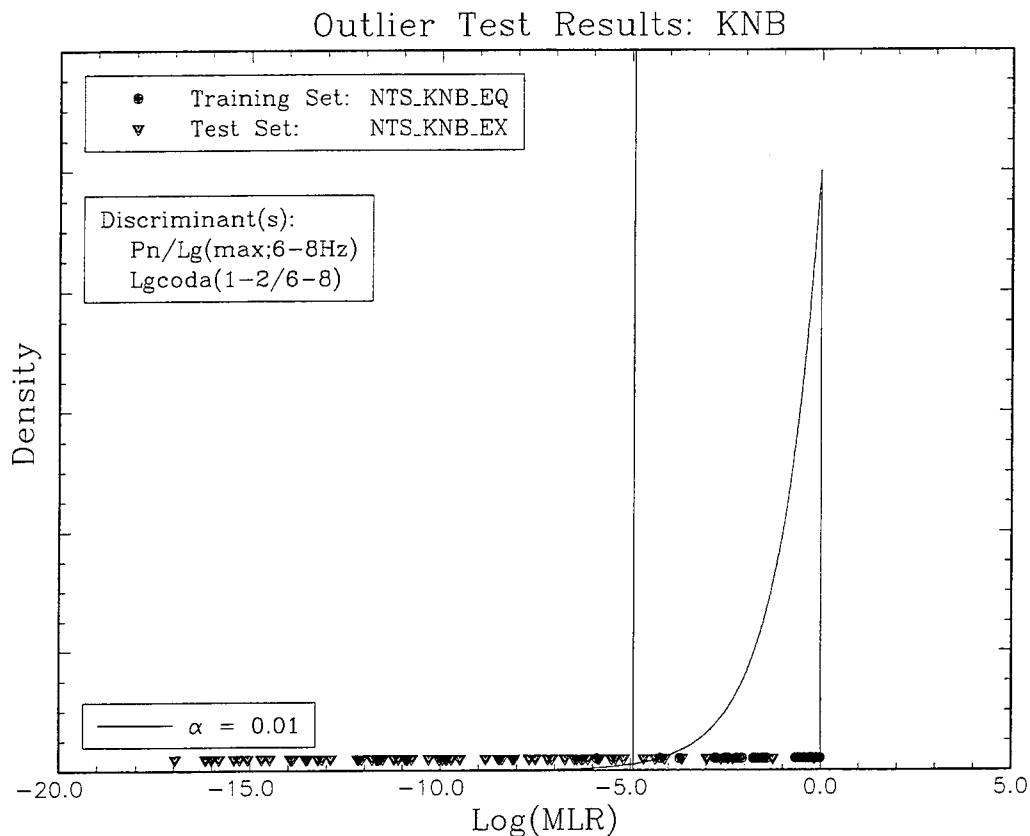


Figure 22. Same as Figure 21 but for events recorded by KNB with both discriminant values present.

## 4.2. Contaminated Training Set Study

We have assumed to this point that the data sets in each region consist of earthquakes and at most one explosion. In practice, data sets will also consist of quarry blasts and rock bursts, but we may not know this a priori. Thus, we should be concerned with the situation in which quarry blasts and rock bursts may contaminate earthquake training sets when trying to detect a nuclear explosion. Although there are likely to be only a small number of quarry blasts above magnitude 3, it is possible that a couple of large quarry blasts might contaminate the earthquake training set. Large ( $m_b > 3$ ) rock bursts or mine tremors could also occur and be present in data sets. The purpose of this study is to determine how a lack of ground-truth affects our ability to monitor using the outlier test.

To address this problem, we intentionally included quarry blasts or rock bursts in earthquake training sets to determine if the outlier test can detect them and to assess potential impacts on identification performance. (Note that in Section 4.1, we considered each quarry blast to be a “new” generic explosion for the sake of estimating a lower bound

on the detection rate of nuclear explosions as outliers for regions in which nuclear explosion data was lacking or minimal. Here we consider the quarry blasts as unique events which can degrade our ability to identify nuclear explosions.)

We first selected 2 Vogtland quarry blasts and inserted them in the Vogtland earthquake set. To make the problem interesting, we chose the 2 that are most like the earthquakes. We then ran the outlier test on each event in the training set using the leave-one-out procedure and the same discriminants as above. Note that even if one quarry blast is left out of the training set to be tested, one contaminating event still remains. If an outlier is detected, it is removed from the set and the remainder are tested again. In this case, both quarry blasts were flagged on the first pass. If the 2 quarry blasts are not removed from the earthquake training set, 2 of the remaining 11 Vogtland quarry blasts are undetected when tested.

This analysis was repeated by randomly selecting 2 Kola Peninsula quarry blasts and inserting them in the Steigen earthquake set. Only one quarry blast was detected on the first pass, but once removed, the other was also detected. If the 2 Kola quarry blasts are not removed from the Steigen earthquake training set, 7 of the remaining 51 quarry blasts are undetected when tested. However, even if both Kola quarry blasts were not detected, the outlier test was still able to detect all 3 Novaya Zemlya nuclear explosions as outliers. (ARCESS was the only array for which we have data of these three types.)

As a related study, we contaminated the Vogtland earthquake set with 30 Lubin rock bursts and then tested the Vogtland quarry blasts. All 13 Vogtland quarry blasts were still flagged as outliers. This is primarily due to the fact that Pn/Lg measurements for the Vogtland quarry blasts are considerably higher than those for the Vogtland earthquakes and Lubin rock bursts (cf. Figure 10).

These results show that the outlier test can be used to detect contaminating events, in proportions of 10–20%, in data sets which lack ground-truth. If they are not detected and contaminated data sets are used to train the outlier test, the probability of detecting an explosion may be degraded significantly, by 15-20% or more, although it did not affect the ability to identify the Novaya Zemlya explosions as outliers. Contamination by rock bursts did not reduce the capability to detect mining explosions as outliers in the case examined, but should be studied more fully.

### 4.3. Applications with the Classification Test

Since we actually have well-defined training sets for more than one event type in the various regions considered, we can use the classification test in these regions to identify new events. Here we perform a study similar to that in Section 4.1 to estimate the rate at which explosions are identified correctly and the false alarm rate. Again we use the leave-one-out procedure, in which each event being tested is sequentially removed from the data sets used to train the classification test. The objectives here are to illustrate how regions can be monitored with the classification test if multiple training sets are available and to assess the improvement in monitoring performance this test offers over the outlier test. The significance level was again set at 0.01. Here we summarize the results of this study.

First, the classification results for ARCESS and GERESS are equivalent to those using the outlier test. For ARCESS, using the Novaya Zemlya explosions and Steigen/Spitsbergen earthquakes to train the test, 3 of 3 Novaya Zemlya explosions and all 29 earthquakes were correctly identified using the distance-corrected discriminants listed in Section 4.1. Similar tests correctly identified all 24 Steigen earthquakes, 50 of 51 (98%) Kola quarry blasts, and 36 of 39 (92%) Kiruna quarry blasts once distance corrections were applied. For GERESS, using the Vogtland earthquakes and quarry blasts to train the classification test, 10 of 10 earthquakes and 13 of 13 quarry blasts were identified correctly. Thus, as before, there were no false alarms at ARCESS or GERESS, while 96% and 100% of the explosions were identified correctly at ARCESS and GERESS, respectively. Four of the 90 quarry blasts are still found to be more consistent with the earthquakes than with the other quarry blasts.

Second, the classification test correctly identified all WMQ event; 23 of 23 earthquakes and 17 of 17 Balapan and Lop Nor nuclear explosions were identified correctly. This is an improvement over the outlier test for which there was one false alarm at WMQ.

Third, the classification test provides greatest improvement over the outlier test for the LNN stations. For MNV, 78 of 78 NTS nuclear explosions and 37 of 37 earthquakes were identified correctly. Recall that the outlier test misidentified 4 of the NTS explosions and 1 of the earthquakes recorded by MNV. For KNB, 75 of 89 (84%) NTS nuclear explosions and 58 of 59 (98%) earthquakes were identified correctly. Note that there was also one false alarm at KNB using the outlier test and 4 additional NTS explosions were misidentified.

Figure 23 illustrates classification results for the events recorded by MNV. The distribution on the right is of the likelihood ratio which was bootstrapped from the earthquake and

explosion training data, and the new event was bootstrapped from the earthquake set. The distribution on the left is similar except that the new event was bootstrapped from the explosion set. The vertical lines correspond to thresholds of the test for various significance levels listed in the lowest legend. The thick vertical line corresponds to the classification rule which minimizes the total error rate. The triangles correspond to values of the likelihood ratio for the explosions being tested, while the circles correspond to similar values for the earthquakes. This plot shows that all events are correctly identified at 0.01 significance level and for the classification rule which minimizes the total error rate.

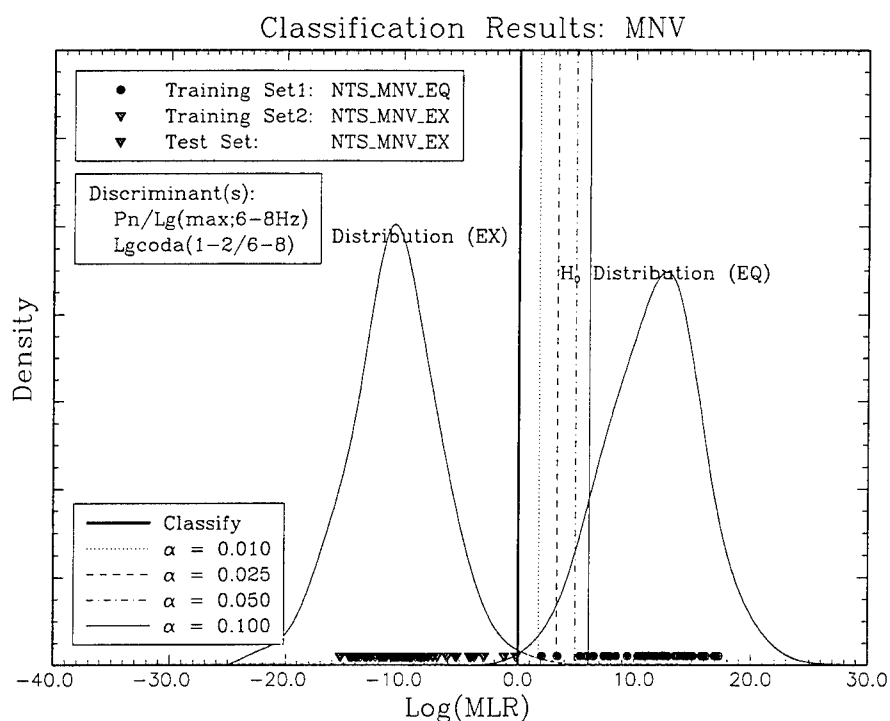


**Figure 23. Graphical representation of classification results for 78 NTS nuclear explosions (triangles) and 37 earthquakes (circles) recorded by MNV. All events were classified correctly.**

Figure 24 illustrates similar classification results for the events recorded by KNB. This plot shows that 75 of 89 (84%) NTS explosions and 58 of 59 earthquakes are classified correctly using the threshold at 0.01 significance level. Plots of the classification results at station WMQ and the ARCESS and GERESS arrays are similar.

The classification results illustrate the improved identification performance of the classification test over the outlier test for regions in which multiple training sets exist. Between 96–100% of the explosions and quarry blasts in the various regions were identified correctly, except at KNB where the identification rate was 84%. Also, there was only one false alarm at KNB using the classification test. Overall, 272 of 290 (94%)

explosions were identified correctly and there was only 1 false alarm out of 158 earthquakes (0.6%), less than the target rate of 1%. Figure 25 summarizes these results.

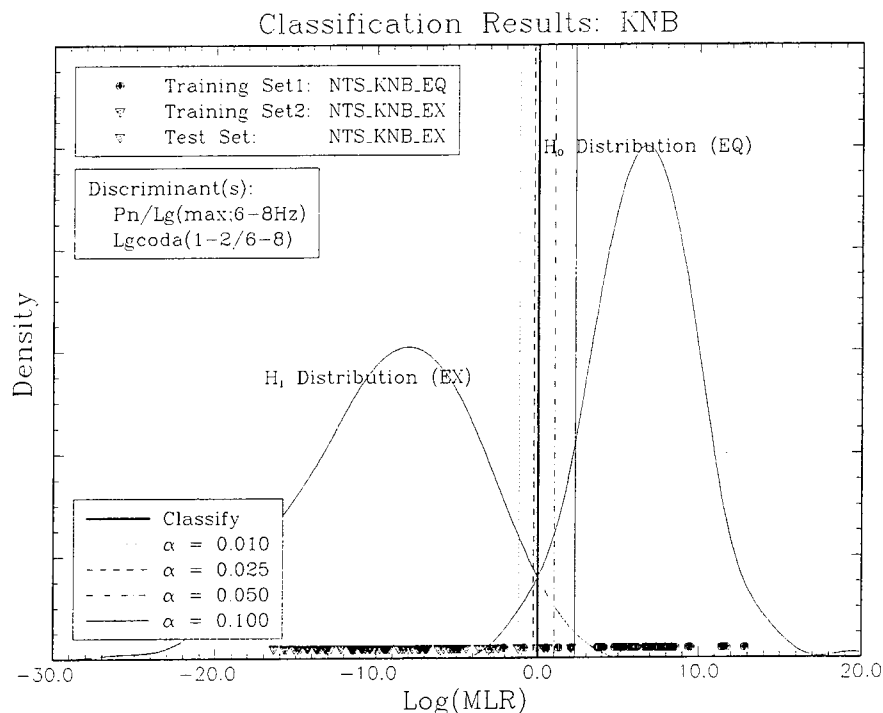


Figure 24. Graphical representation of classification results for 89 NTS nuclear explosions (triangles) and 59 earthquakes (circles) recorded by KNB. In this case, 75 of 89 explosions and 58 of 59 earthquakes were classified correctly at 0.01 significance level.

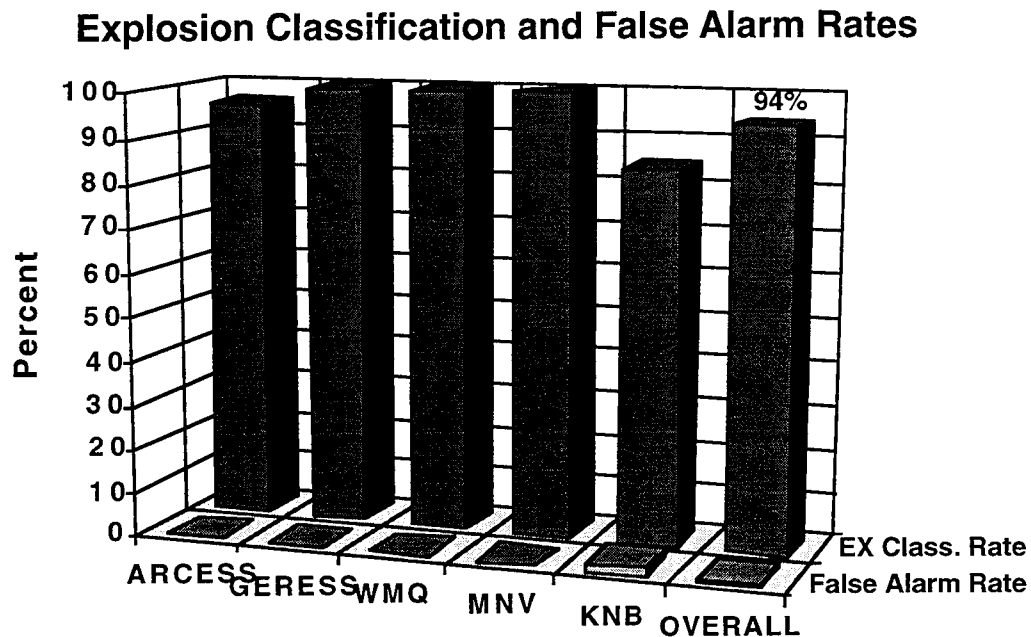


Figure 25. Summary of classification results at ARCESS, GERESS, WMQ, MNV and KNB. Results are expressed in terms of the percentage of explosions correctly classified and the false alarm rate at each station. Overall results are shown on the far right.

#### **4.4. Identification Results for the 921231 Novaya Zemlya Event**

Here we examine the identification of the 31 December 1992 (921231) event on Novaya Zemlya as a special case. Based on origin analysis by the Intelligent Monitoring System (e.g., Bache et al., 1990), a small regional event ( $M_L$  2.26) occurred at origin time 12/31/92 09:29:24 (GMT), latitude 73.58 and longitude 55.21 on Novaya Zemlya. (This event is also referred to by its origin identification number 361575.) Considerable interest in this event is motivated by its relevance to future CTBT or NPT monitoring scenarios since it occurred in an area of very low seismicity, had magnitude corresponding to a fully decoupled 1 kt nuclear test, and was detected by only a few arrays at regional distances (Ryall, 1993). Of further interest is the fact that it occurred in a region where previous underground nuclear tests had been conducted.

Several ARPA contractors previously analyzed the identification of the 921231 event and their results are summarized by Ryall (1993). They generally agreed that this event was not a nuclear detonation. Results obtained by Baumgardt (1993b), Fisk and Gray (1993), and Pulli and Dysart (1993) suggest that this event was much more like Kola Peninsula mining blasts than earthquakes in Scandinavia and near Spitsbergen, in apparent contradiction to a statement by the Seismological Service of the Ministry of Defense, Russian Federation, that no blasting had occurred on the Novaya Zemlya test range on the day in question (Ryall, 1993).

Discriminants used to obtain the previous results were based on Pn and Sn measurements of ARCESS recordings. No corrections were made for attenuation, although all authors recognized their importance on the outcome of identification tests since the epicentral distances of the 921231 event and reference events ranged from 300 to 1300 km and it is well known Pn/Sn is affected by distance. More rapid attenuation of Sn with distance relative to Pn would cause the 921231 event to have higher Pn/Sn ratios than a similar event occurring in the Steigen or Kola Peninsula regions due to the longer path from Novaya Zemlya. It was speculated that applying distance corrections may lead to Pn/Sn ratios that are more consistent with earthquakes than with quarry blasts.

The objectives of this study are to resolve the apparent discrepancy and to assess the impact of attenuation on regional event identification. Using distance corrections reported by Sereno (1990), we reanalyzed the identification of the 921231 event. As in the study by Fisk and Gray (1993), the feature data used here were obtained from seismic analysis performed by Baumgardt (1993b) using the Intelligent Seismic Event Identification System



(ISEIS) (e.g., Baumgardt et al., 1991). Discriminants consist of Pn/Sn ratios of maximum amplitude measurements in five frequency bands, 4-6, 5-7, 6-8, 8-10, and 8-16 Hz recorded by ARA0. For comparison, we again used 3 nuclear explosions at the Novaya Zemlya test site, the Kola and Steigen data sets, and 5 earthquakes near Spitsbergen. Figure 26 shows the locations of these events and the ARCESS array. Figure 9 above shows scatter plots of the Pn/Sn measurements for these events before and after applying distance corrections.

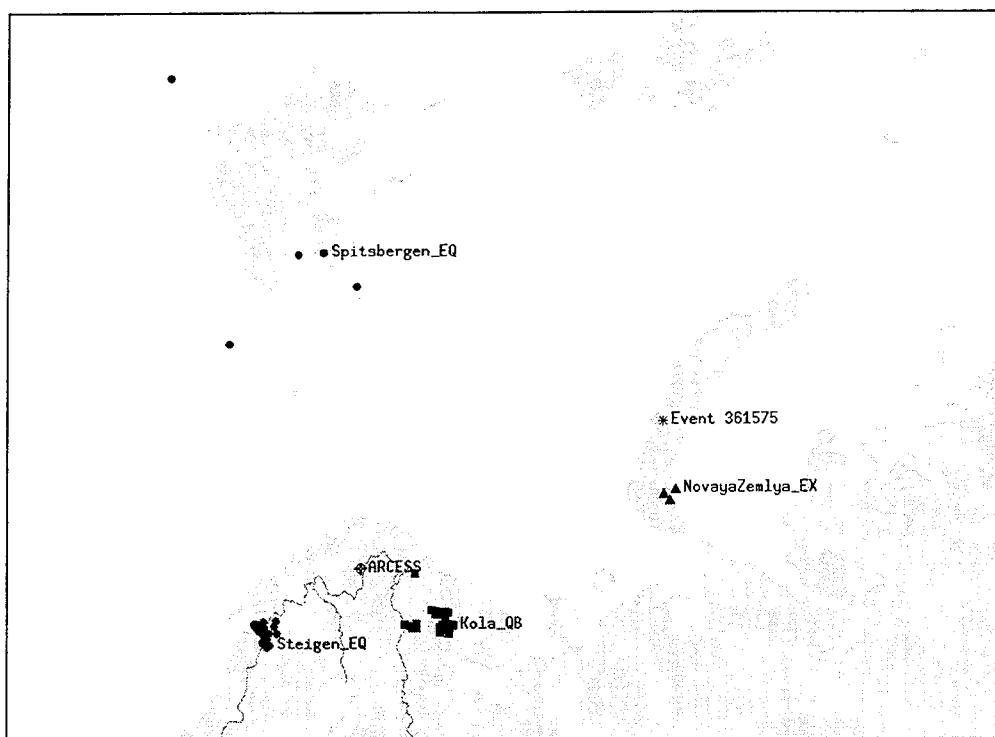


**Figure 26.** Locations of the 921231 event (ORID=361575) on Novaya Zemlya, reference events used in its identification analysis, and the ARCESS array at which all events were recorded.

After first applying distance corrected to these discriminants, we applied the outlier and classification tests to the 921231 event. Since there are training data for three groups in this region, (i.e., for nuclear explosions, earthquakes and mining blasts) the classification test was used to allocate the 921231 event into one of them. The outlier test was also used to illustrate how it would be applied to identifying this event if only any one of the three training sets existed. We also examined the range of significance levels for which various hypothesis are rejected. This type of in-depth analysis using multiple tests illustrates how an expert analyst might use these tools in an interactive mode to examine suspicious or problematic events. The following results and observations were obtained. (Further details are provided by Fisk, 1993.)

First, there is sufficient evidence to reject the 921231 event as a member of the Novaya Zemlya nuclear explosion group at 0.01 significance level, using either the outlier or classification tests. This is consistent with the results of Fisk and Gray (1993) as expected since the epicentral distances for the Novaya Zemlya events are all very similar; thus, attenuation corrections should have little effect on the identification relative to this group.

Second, based on separate outlier tests, there is insufficient evidence to reject the 921231 event as a member of either the quarry blast or earthquake groups at 0.05 significance level or below. Thus, using the monitoring procedure described in Section 3.2, this event would not be flagged as an outlier for further analysis based solely on Pn/Sn measurements. However, it would be flagged as an outlier if we included the seismicity of Novaya Zemlya as a discrimination parameter since the seismicity of this region is very low. Furthermore, there is no commercial mining activity on Novaya Zemlya while there is a nuclear test site.

Third, classification between earthquake and quarry blast alternatives led to rejection of this event as a member of the Kola quarry blast group at 0.05 significance level, although it was also rejected as a member of the earthquake group using Pn/Sn in the five frequency bands. Omitting the 6-8 Hz band (which was found to be inconsistent with the values in the other four bands for the 921231 event), it was rejected as a quarry blast at 0.01 significance level and accepted as an earthquake. These results are quite different than those of Fisk and Gray (1993), Baumgardt (1993b) and Pulli and Dysart (1993), who found that the 921231 event was much more consistent with identification as a mining blast than as an earthquake. Although identification of this event is still somewhat inconclusive, due to its Pn/Sn value in the 6-8 Hz band, it is no longer inconsistent with the statement by the Seismological Service of the Ministry of Defense, Russian Federation. This study also demonstrates that distance corrections can have a significant impact on event identification and should be applied routinely.

Among other important monitoring issues, we found that distance-corrected Pn/Sn values for the 3 Novaya Zemlya nuclear tests fall well within the values for the Kola quarry blast group (cf. Figure 9). Even uncorrected values are equivalent to those of quarry blasts, except for the bands above 8 Hz. This implies that a more effective discriminator between nuclear explosions and mining blasts is needed. Spectral and cepstral variances, presence of cepstral peaks, and presence of Rg have been considered to identify mining blasts, but adequate utility of any is yet to be demonstrated.

We also found that overlapping or adjacent bands of high-frequency Pn/Sn, based on maximum amplitude measurements, can provide different evidence. In this case, Pn/Sn in the 6-8 Hz band was anomalously higher than in the other bands for the 921231 event (Figure 9). This may indicate that a more robust type of Pn/Sn measurement is needed.

## 5. Conclusions and Recommendations

Results presented in Section 4.1 show that useful monitoring can be performed with the outlier-detection approach, currently down to magnitude 3, for regions that are well-covered by at least one seismic station or array. Using Pn/Lg and Pn/Sn in several 3-8 Hz bands, between 92–100% of the explosions and quarry blasts were detected as outliers of the earthquake groups in the various regions, except at KNB where the detection rate was 80%. (An Lg spectral ratio was also used at KNB and MNV since we only had Pn/Lg in the 6-8 Hz band for these events.) There were no false alarms at ARCESS or GERESS, while there was one false alarm at each of KNB, MNV and WMQ. Overall, 264 of 290 (91%) explosions were detected and there were only 3 false alarms out of 158 earthquakes (1.9%), slightly higher than the target rate of 1%. These results were obtained for diverse regions, for a wide range of epicentral distances and magnitudes, and for single stations and arrays.

Although these preliminary results are encouraging for monitoring down to magnitude 3, improvements are still needed. The relatively high detection rate of explosions as outliers should provide a useful deterrent to potential clandestine testing. From a monitoring perspective, however, it is desired that all underground nuclear tests be identified. In addition, the false alarm rate is relatively low and could be set even lower. This greatly alleviates the burden on human analysts. In practice, however, there will be many more earthquakes to contend with than the number considered in this study, with a corresponding percentage identified as outliers. Although a false alarm by the outlier test would not necessitate an on-site inspection, for example (these would simply be included with a set of events to be examined in more detail), it is important to reduce the false alarm rate further while maintaining a high detection rate of explosions as outliers.

One or more additional discriminants that work about as well as high-frequency Pn/Sn and Pn/Lg, but that are relatively uncorrelated, or information which allows us to choose the best discriminants and frequency bands in a given region, should improve regional identification performance further. Although Lg spectral ratios discriminate in some regions (e.g., the western U.S. and Germany), they do not in others (e.g., Scandinavia and

Eurasia). Thus, we are hesitant to use them in an operational setting until further physical understanding of where and why they discriminate is obtained.

Contaminated training data did not reduce the monitoring capability for the cases studied but remains a cause for concern, especially at low magnitude. We also found that it is very important to distance-correct discriminants in order to obtain accurate identification results. Examples were shown in which the 880929 Lop Nor explosion and the 921231 Novaya Zemlya event would be misidentified using discriminants uncorrected for distance. Transporting regional discrimination rules appears very difficult and must be done very precisely in order to have a reasonable probability of detecting a nuclear explosion as an outlier without having an unmanageable number of false alarms worldwide. A key benefit of the outlier approach is that it does not require transporting discrimination thresholds, while providing high outlier-detection and low false alarm rates in regions studied thus far.

Results presented in Section 4.3 show that the classification test provides improved identification accuracy over the outlier test for cases in which well-defined training sets are available for more than one type of event. Between 96–100% of the explosions and quarry blasts in the various regions were identified correctly, except at KNB where the identification rate of NTS nuclear explosions was 84%. Also, there was only one false alarm which occurred at KNB using the classification test. Overall, 272 of 290 (94%) explosions were identified correctly and there was only 1 false alarms out of 158 earthquakes (0.6%), less than the target rate of 1%. These results illustrate how the classification test could be used to monitor existing nuclear test sites, for example, with very high identification accuracy.

Future research should focus on investigating ways to select the best regional discriminants in the absence of nuclear explosion training data and on investigating other discriminants such a regional  $M_s$ - $m_b$  for  $m_b < 4$  (e.g., Dainty and Kushnir, 1994; Herrin et al., 1994), a discriminant of earthquakes and explosions based on autoregression analysis of  $L_g$  (e.g., Herrin et al., 1994), waveform complexity (e.g. Blandford, 1993), etc. In addition, reliable automated methods are needed to distinguish nuclear explosions from chemical mining blasts, particularly to improve the seismic monitoring capability below magnitude 3. Last, a distance-correction data base should be established.

## References

- Bache, T.C., S.R. Bratt, J. Wang, R.M. Fung, C. Kobryn and J.W. Given (1990). The Intelligent Monitoring System, *Bull. Seism. Soc. Am.*, **80**, 1833-1851.
- Baek, J., H.L. Gray, and W.A. Woodward (1992). A Generalized Likelihood Ratio Test in Outlier Detection or Script Matching, Technical Report, Department of Statistical Science, Southern Methodist University, Dallas, TX.
- Baek, J., H.L. Gray, W.A. Woodward and M.D. Fisk (1993). A Bootstrap Generalized Likelihood Ratio Test in Discriminant Analysis, submitted to *Comp. Stat. and Data Anal.*, Southern Methodist University, Dallas, TX.
- Baumgardt, D.R. (1994). Regional Characterization of Mine Blasts, Earthquakes, Mine Tremors, and Nuclear Explosions Using the Intelligent Seismic Event Identification System, Technical Report SAS-TR-94-12, ENSCO, Inc., Springfield, VA.
- Baumgardt, D.R. (1993a). Private Communication.
- Baumgardt, D.R. (1993b). Seismic waveform feature analysis and discrimination of the December 31, 1992 Novaya Zemlya event, Paper in volume compiled by Ryall (1993).
- Baumgardt, D.R. (1990). Investigation of teleseismic Lg blockage and scattering using NORESS and ARCESS regional arrays, *Bull. Seism. Soc. Am.*, **80**, 2261-2281.
- Baumgardt, D.R., J. Carney, M. Maxson and S. Carter (1992). Evaluation of Regional Discriminants using the Intelligent Seismic Event Identification System, Semi-Annual Technical Report SAS-TR-93-38, ENSCO, Inc., Springfield, VA.
- Baumgardt, D.R. and Z. Der (1994). Performance and Portability of Regional Seismic Waveform Discriminants in Different Tectonic Regions, in *Proceeding of the 16th Annual Seismic Research Symposium*, 7-9 September 1994, Thornwood, NY, PL-TR-2217, Phillips Laboratory, Hanscom AFB, MA, ADA284667.
- Baumgardt, D.R., G. Young and K. Ziegler (1991). Design and Development of the Intelligent Seismic Event Identification System: Design Considerations and Processing for Regional Event Identification, Technical Report PL-TR-91-2211, Phillips Laboratory, Hanscom AFB, MA, ADA246793.
- Bennett, T.J., B.W. Barker, K.L. McLaughlin and J.R. Murphy (1989). Regional Discrimination of Quarry Blasts, Earthquakes, and Underground Nuclear Explosions, GL-TR-89-0114, Hanscom AFB, MA.
- Blandford, R.R., A. Dainty, R. Lacoss, R. Maxion, A. Ryall, B. Stump, C. Thurber, and T. Wallace (1992). Report on the DARPA Seismic Identification Workshop, Center for Seismic Studies, Arlington, VA, 18-19 May 1992.
- Blandford, R. R. (1993). Discrimination of Earthquakes and Explosions at Regional Distances using Complexity, AFTAC-TR-93-044, HQ AFTAC/TTT, Patrick AFB, FL.
- Dainty, A.M. and A.F. Kushnir (1994). Enhancing Surface Wave Signals Using the Undistorting Group Filter, *Proceedings of the 16th Annual Seismic Research Symposium*, PL-TR-94-2217, Hanscom AFB, MA, ADA284667.
- Efron, B. (1979). Bootstrap methods: another look at the jackknife, *Ann. Stat.*, **7**, 1-26.

- Fisk, M.D. (1993). Event Identification Analysis of the 31 December 1992 Novaya Zemlya Event with Attenuation Corrections, MRC-R-1459, Mission Research Corp., Santa Barbara, CA.
- Fisk, M.D. and H.L. Gray (1993). Event Identification Analysis of the Novaya Zemlya Event on 31 December 1992 using Outlier and Classification Likelihood Ratio Tests, Paper in volume compiled by Ryall (1993), MRC-R-1449, Mission Research Corp., Santa Barbara, CA.
- Fisk, M.D., H.L. Gray and G.D. McCartor (1993a). Applications of Generalized Likelihood Ratio Tests to Seismic Event Identification, PL-TR-93-2221, Phillips Laboratory, Hanscom AFB, MA, ADA279479.
- Fisk, M.D., H.L. Gray and W.A. Woodward (1993b). Development of a Robust Statistical Framework for Seismic Event Identification: The Multivariate Statistical EventID Analysis System (MSEAS), MRC-R-1451, Mission Research Corp., Santa Barbara, CA.
- Grant, L., J. Coyne and F. Ryall (1993). CSS Ground-Truth Database: Version 1 Handbook, Technical Report C93-05, Science Applications International Corp., Center for Seismic Studies, Arlington, VA.
- Gray, H.L., W. Woodward, M.D. Fisk and G.D. McCartor (1994). A hypothesis testing approach to discriminant analysis with mixed categorical and continuous variables when data are missing, *Proceeding of the 16th Annual Seismic Research Symposium*, PL-TR-94-2217, Phillips Laboratory, Hanscom AFB, MA, ADA284667.
- Harjes, H.-P. (1990). Design and siting of a new regional seismic array in central Europe, *Bull. Seism. Soc. Am.*, **80**, 1801-1817.
- Hedlin, M.A.H., J.B. Minster and J.A. Orcutt (1990). An automatic means to discriminate between earthquakes and quarry blasts, *Bull. Seism. Soc. Am.*, **80**, 2143-2160.
- Herrin, E., V. Burlacu, H.L. Gray, J. Swanson, P. Golden and B. Myers (1994). Research in Regional Event Discrimination Using Ms:mb and Autoregressive Modeling of Lg Waves, *Proceedings of the 16th Annual Seismic Research Symposium*, PL-TR-94-2217, Hanscom AFB, MA, ADA284667.
- Lay, T. and T. Zhang (1994). Calibration of Regional Wave Discriminants in Diverse Geological Environments: Topographic Correlations, *Proceedings of the 16th Annual Seismic Research Symposium*, PL-TR-94-2217, Hanscom AFB, MA, ADA284667.
- Lilwall, R.C. and A. Douglas (1985). AWRE Report O 23/84 (U.K. Atomic Weapons Research Establishment).
- Meremonte et al. (1994). Constraints on the June 29, 1992 Little Skull Mountain, Nevada earthquake sequence provided by accurate hypocenter estimates, submitted to *Bull. Seism. Soc. Am.*
- Mykkeltveit, S., F. Ringdal, T. Kvaerna and R.W. Alewine (1990). Application of regional arrays in seismic verification, *Bull. Seism. Soc. Am.*, **80**, 1777-1800.
- Patton, H. and W. Walter (1994). Private Communication.

- Pulli, J.J. and P.S. Dysart (1993). Identification analysis of the Dec. 31, 1992 Novaya Zemlya event, Paper in volume compiled by Ryall (1993).
- Ringdal, F. (1984). in The VELA Program: A Twenty-Five Year Review of Basic Research (Ed. A.U. Kerr, Executive Graphic Services), p. 611.
- Ryall, A. (1993). The Novaya Zemlya Event of 31 December 1992 and Seismic Identification Issues, Supplemental volume of papers to Proceedings of the 15th Annual Seismic Research Symposium, 8-10 September 1993, Vail, CO, PL-TR-93-2160, ADA271458.
- Sereno, T.J. (1990). Attenuation of Regional Phases in Fennoscandia and Estimates of Arrival Time and Azimuth Uncertainty using Data Recorded by Regional Arrays, SAIC-90/1472, Science Applications International Corp., San Diego, CA.
- Smith, K.D. and J.N. Brune (1993). A sequence of very shallow earthquakes in the Rock Valley fault zone; southern Nevada Test Site (abstract), *EOS Suppl.*, **74**, 417.
- Taylor, S.R., M.D. Denny, E.S. Vergino and R.E. Glaser (1989). Regional discrimination between NTS explosions and western U.S. earthquakes, *Bull. Seism. Soc. Am.*, **79**, 1142.
- Walter, W.R., K.M. Mayeda and H.J. Patton (1994). Phase and spectral ratio discrimination between NTS earthquakes and explosions Part I: Empirical observations, LLNL Preprint UCRL-JC-118551, submitted to *Bull. Seism. Soc. Am.*

Prof. Thomas Ahrens  
Seismological Lab, 252-21  
Division of Geological & Planetary Sciences  
California Institute of Technology  
Pasadena, CA 91125

Prof. Keiiti Aki  
Center for Earth Sciences  
University of Southern California  
University Park  
Los Angeles, CA 90089-0741

Prof. Shelton Alexander  
Geosciences Department  
403 Deike Building  
The Pennsylvania State University  
University Park, PA 16802

Dr. Thomas C. Bache, Jr.  
Science Applications Int'l Corp.  
10260 Campus Point Drive  
San Diego, CA 92121 (2 copies)

Prof. Muawia Barazangi  
Cornell University  
Institute for the Study of the Continent  
3126 SNEE Hall  
Ithaca, NY 14853

Dr. Douglas R. Baumgardt  
ENSCO, Inc  
5400 Port Royal Road  
Springfield, VA 22151-2388

Dr. T.J. Bennett  
S-CUBED  
A Division of Maxwell Laboratories  
11800 Sunrise Valley Drive, Suite 1212  
Reston, VA 22091

Dr. Robert Blandford  
AFTAC/TT, Center for Seismic Studies  
1300 North 17th Street  
Suite 1450  
Arlington, VA 22209-2308

Dr. Steven Bratt  
ARPA/NMRO  
3701 North Fairfax Drive  
Arlington, VA 22203-1714

Dale Breiding  
U.S. Department of Energy  
Recipient, IS-20, GA-033  
Office of Arms Control  
Washington, DC 20585

Dr. Jerry Carter  
Center for Seismic Studies  
1300 North 17th Street  
Suite 1450  
Arlington, VA 22209-2308

Mr Robert Cockerham  
Arms Control & Disarmament Agency  
320 21st Street North West  
Room 5741  
Washington, DC 20451,

Dr. Zoltan Der  
ENSCO, Inc.  
5400 Port Royal Road  
Springfield, VA 22151-2388

Dr. Stanley K. Dickinson  
AFOSR/NM  
110 Duncan Avenue  
Suite B115  
Bolling AFB, DC

Dr Petr Firbas  
Institute of Physics of the Earth  
Masaryk University Brno  
Jecna 29a  
612 46 Brno, Czech Republic

Dr. Mark D. Fisk  
Mission Research Corporation  
735 State Street  
P.O. Drawer 719  
Santa Barbara, CA 93102

Dr. Cliff Frolich  
Institute of Geophysics  
8701 North Mopac  
Austin, TX 78759

Dr. Holly Given  
IGPP, A-025  
Scripps Institute of Oceanography  
University of California, San Diego  
La Jolla, CA 92093

Dr. Jeffrey W. Given  
SAIC  
10260 Campus Point Drive  
San Diego, CA 92121

Dr. Dale Glover  
Defense Intelligence Agency  
ATTN: ODT-1B  
Washington, DC 20301



Dan N. Hagedorn  
Pacific Northwest Laboratories  
Battelle Boulevard  
Richland, WA 99352

Robert C. Kemerait  
ENSCO, Inc.  
445 Pineda Court  
Melbourne, FL 32940

Dr. James Hannon  
Lawrence Livermore National Laboratory  
P.O. Box 808, L-205  
Livermore, CA 94550

U.S. Dept of Energy  
Max Koontz, NN-20, GA-033  
Office of Research and Develop.  
1000 Independence Avenue  
Washington, DC 20585

Dr. Roger Hansen  
University of Colorado, JSPC  
Campus Box 583  
Boulder, CO 80309

Dr. Richard LaCoss  
MIT Lincoln Laboratory, M-200B  
P.O. Box 73  
Lexington, MA 02173-0073

Prof. David G. Harkrider  
Division of Geological & Planetary Sciences  
California Institute of Technology  
Pasadena, CA 91125

Prof. Charles A. Langston  
Geosciences Department  
403 Deike Building  
The Pennsylvania State University  
University Park, PA 16802

Prof. Danny Harvey  
University of Colorado, JSPC  
Campus Box 583  
Boulder, CO 80309

Jim Lawson, Chief Geophysicist  
Oklahoma Geological Survey  
Oklahoma Geophysical Observatory  
P.O. Box 8  
Leonard, OK 74043-0008

Prof. Donald V. Helmberger  
Division of Geological & Planetary Sciences  
California Institute of Technology  
Pasadena, CA 91125

Prof. Thorne Lay  
Institute of Tectonics  
Earth Science Board  
University of California, Santa Cruz  
Santa Cruz, CA 95064

Prof. Eugene Herrin  
Geophysical Laboratory  
Southern Methodist University  
Dallas, TX 75275

Dr. William Leith  
U.S. Geological Survey  
Mail Stop 928  
Reston, VA 22092

Prof. Robert B. Herrmann  
Department of Earth & Atmospheric Sciences  
St. Louis University  
St. Louis, MO 63156

Mr. James F. Lewkowicz  
Phillips Laboratory/GPE  
29 Randolph Road  
Hanscom AFB, MA 01731-3010( 2 copies)

Prof. Lane R. Johnson  
Seismographic Station  
University of California  
Berkeley, CA 94720

Dr. Gary McCartor  
Department of Physics  
Southern Methodist University  
Dallas, TX 75275

Prof. Thomas H. Jordan  
Department of Earth, Atmospheric &  
Planetary Sciences  
Massachusetts Institute of Technology  
Cambridge, MA 02139

Prof. Thomas V. McEvilly  
Seismographic Station  
University of California  
Berkeley, CA 94720

Dr. Keith L. McLaughlin  
S-CUBED  
A Division of Maxwell Laboratory  
P.O. Box 1620  
La Jolla, CA 92038-1620

Prof. Bernard Minster  
IGPP, A-025  
Scripps Institute of Oceanography  
University of California, San Diego  
La Jolla, CA 92093

Prof. Brian J. Mitchell  
Department of Earth & Atmospheric Sciences  
St. Louis University  
St. Louis, MO 63156

Mr. Jack Murphy  
S-CUBED  
A Division of Maxwell Laboratory  
11800 Sunrise Valley Drive, Suite 1212  
Reston, VA 22091 (2 Copies)

Dr. Keith K. Nakanishi  
Lawrence Livermore National Laboratory  
L-025  
P.O. Box 808  
Livermore, CA 94550

Prof. John A. Orcutt  
IGPP, A-025  
Scripps Institute of Oceanography  
University of California, San Diego  
La Jolla, CA 92093

Dr. Howard Patton  
Lawrence Livermore National Laboratory  
L-025  
P.O. Box 808  
Livermore, CA 94550

Dr. Frank Pilotte  
HQ AFTAC/TT  
1030 South Highway A1A  
Patrick AFB, FL 32925-3002

Dr. Jay J. Pulli  
Radix Systems, Inc.  
201 Perry Parkway  
Gaithersburg, MD 20877

Prof. Paul G. Richards  
Lamont-Doherty Earth Observatory  
of Columbia University  
Palisades, NY 10964

Mr. Wilmer Rivers  
Multimax Inc.  
1441 McCormick Drive  
Landover, MD 20785

Dr. Alan S. Ryall, Jr.  
Lawrence Livermore National Laboratory  
L-025  
P.O. Box 808  
Livermore, CA 94550

Dr. Chandan K. Saikia  
Woodward Clyde- Consultants  
566 El Dorado Street  
Pasadena, CA 91101

Mr. Dogan Seber  
Cornell University  
Inst. for the Study of the Continent  
3130 SNEE Hall  
Ithaca, NY 14853-1504

Secretary of the Air Force  
(SAFRD)  
Washington, DC 20330

Office of the Secretary of Defense  
DDR&E  
Washington, DC 20330

Thomas J. Sereno, Jr.  
Science Application Int'l Corp.  
10260 Campus Point Drive  
San Diego, CA 92121

Dr. Michael Shore  
Defense Nuclear Agency/SPSS  
6801 Telegraph Road  
Alexandria, VA 22310

Prof. David G. Simpson  
IRIS, Inc.  
1616 North Fort Myer Drive  
Suite 1050  
Arlington, VA 22209

Dr. Jeffrey Stevens  
S-CUBED  
A Division of Maxwell Laboratory  
P.O. Box 1620  
La Jolla, CA 92038-1620

Prof. Brian Stump  
Los Alamos National Laboratory  
EES-3  
Mail Stop C-335  
Los Alamos, NM 87545

TACTEC  
Battelle Memorial Institute  
505 King Avenue  
Columbus, OH 43201 (Final Report)

Prof. Tuncay Taymaz  
Istanbul Technical University  
Dept. of Geophysical Engineering  
Mining Faculty  
Maslak-80626, Istanbul Turkey

Phillips Laboratory  
ATTN: GPE  
29 Randolph Road  
Hanscom AFB, MA 01731-3010

Prof. M. Nafi Toksoz  
Earth Resources Lab  
Massachusetts Institute of Technology  
42 Carleton Street  
Cambridge, MA 02142

Phillips Laboratory  
ATTN: TSML  
5 Wright Street  
Hanscom AFB, MA 01731-3004

Dr. Larry Turnbull  
CIA-OSWR/NED  
Washington, DC 20505

Phillips Laboratory  
ATTN: PL/SUL  
3550 Aberdeen Ave SE  
Kirtland, NM 87117-5776 (2 copies)

Dr. Karl Veith  
EG&G  
5211 Auth Road  
Suite 240  
Suitland, MD 20746

Dr. Michel Campillo  
Observatoire de Grenoble  
I.R.I.G.M.-B.P. 53  
38041 Grenoble, FRANCE

Prof. Terry C. Wallace  
Department of Geosciences  
Building #77  
University of Arizona  
Tucson, AZ 85721

Dr. Kin Yip Chun  
Geophysics Division  
Physics Department  
University of Toronto  
Ontario, CANADA

Dr. William Wortman  
Mission Research Corporation  
8560 Cinderbed Road  
Suite 700  
Newington, VA 22122

Prof. Hans-Peter Harjes  
Institute for Geophysic  
Ruhr University/Bochum  
P.O. Box 102148  
4630 Bochum 1, GERMANY

ARPA, OASB/Library  
3701 North Fairfax Drive  
Arlington, VA 22203-1714

Prof. Eystein Husebye  
NTNF/NORSAR  
P.O. Box 51  
N-2007 Kjeller, NORWAY

HQ DNA  
ATTN: Technical Library  
Washington, DC 20305

David Jepsen  
Acting Head, Nuclear Monitoring Section  
Bureau of Mineral Resources  
Geology and Geophysics  
G.P.O. Box 378, Canberra, AUSTRALIA

Defense Technical Information Center  
Cameron Station  
Alexandria, VA 22314 (2 Copies)

Ms. Eva Johannisson  
Senior Research Officer  
FOA  
S-172 90 Sundbyberg, SWEDEN

Dr. Peter Marshall  
Procurement Executive  
Ministry of Defense  
Blacknest, Brimpton  
Reading FG7-FRS, UNITED KINGDOM

Dr. Bernard Massinon, Dr. Pierre Mechler  
Societe Radiomana  
27 rue Claude Bernard  
75005 Paris, FRANCE (2 Copies)

Dr. Svein Mykkeltveit  
NTNT/NORSAR  
P.O. Box 51  
N-2007 Kjeller, NORWAY (3 Copies)

Dr. Jorg Schlittenhardt  
Federal Institute for Geosciences & Nat'l Res.  
Postfach 510153  
D-30631 Hannover , GERMANY

Dr. Johannes Schweitzer  
Institute of Geophysics  
Ruhr University/Bochum  
P.O. Box 1102148  
4360 Bochum 1, GERMANY

Trust & Verify  
VERTIC  
Carrara House  
20 Embankment Place  
London WC2N 6NN, ENGLAND